JGR Biogeosciences

RESEARCH ARTICLE
10.1029/2022JG006831

Riparian Microtopography Affects Event-Driven Stream DOC Concentrations and DOM Quality in a Forested Headwater Catchment

Katharina Blaurock[1], Phil Garthen[1], Maria P. da Silva[2], Burkhard Beudert[3], Benjamin S. Gilfedder[1], Jan H. Fleckenstein[4,5], Stefan Peiffer[1], Oliver J. Lechtenfeld[2,6], and Luisa Hopp[1]

[1]Department of Hydrology, Bayreuth Center of Ecology and Environmental Research (BayCEER), University of Bayreuth, Bayreuth, Germany, [2]Department of Analytical Chemistry, Research Group BioGeoOmics, Helmholtz Centre for Environmental Research - UFZ, Leipzig, Germany, [3]Department of Nature Conservation and Research, Bavarian Forest National Park, Grafenau, Germany, [4]Department of Hydrogeology, Helmholtz Centre for Environmental Research - UFZ, Leipzig, Germany, [5]Hydrological Modelling Unit, Bayreuth Center of Ecology and Environmental Research (BayCEER), University of Bayreuth, Bayreuth, Germany, [6]ProVIS - Centre for Chemical Microscopy, Helmholtz Centre for Environmental Research - UFZ, Leipzig, Germany

Abstract The transport of dissolved organic carbon (DOC) from the soils to inland waters plays an important role in the global carbon cycle. Widespread increases in DOC concentrations have been observed in surface waters over the last few decades, affecting carbon balances, ecosystem functioning and drinking water treatment. However, the primary hydrological controls on DOC mobilization are still uncertain. The aim of this study was to investigate the role of microtopography in the riparian zone for DOC export and DOM quality. DOC concentration and DOM quality in the shallow groundwater of a riparian zone and in streamflow in a forested headwater catchment was investigated using fluorescence and absorbance characteristics. We found higher DOC concentrations with a higher aromaticity in the microtopographical depressions, which were influenced by highly dynamic shallow groundwater levels, than in the flat forest soil. As a result of the frequent wet-dry cycles in the upper soil layers, aromatic DOC accumulated in the shallow groundwater within and below the microtopographical depressions. Rising groundwater levels during precipitation events led to the connection of the microtopographical depressions to the stream, resulting in a change toward more aromatic DOC in the stream. Increasing stream DOC concentrations were accompanied by increasing concentrations of iron and aluminum, suggesting the coupled release of these metals with DOC from the riparian zone. Our results highlight the importance of the interplay between microtopography and groundwater level dynamics in the riparian zone for DOC export from headwater catchments.

Plain Language Summary Dissolved organic carbon (DOC) is the result of the continuous breakdown of organic material, such as leaves. It accumulates in the soil and is transported to streams mainly during precipitation events. In this study, we analyzed the shallow groundwater of two differing sites in the Bavarian Forest National Park. Both sites were located close to the stream, but one was characterized by typical forest soil and one by small ponds, which were occasionally filled with water. The site with ponds showed much higher DOC concentrations and the DOC was chemically different from the other site. During a precipitation event, we observed a shift in chemical composition of stream water parameters toward the chemical characteristics found at the site with ponds. Therefore, we conclude that the ponds contribute substantially to DOC mobilization, once they fill with water and get connected to the stream.

Key Points:

- This study found small-scale differences in dissolved organic carbon (DOC) concentrations and dissolved organic matter (DOM) quality in the riparian zone
- Microtopographical depressions were characterized by high DOC concentrations and aromatic DOC
- In-stream DOC concentrations and DOM quality during a precipitation event resembled shallow groundwater below microtopographical depressions

Supporting Information:

Supporting Information may be found in the online version of this article.

Correspondence to:

K. Blaurock,
katharina.blaurock@uni-bayreuth.de

Citation:

Blaurock, K., Garthen, P., da Silva, M. P., Beudert, B., Gilfedder, B. S., Fleckenstein, J. H., et al. (2022). Riparian microtopography affects event-driven stream DOC concentrations and DOM quality in a forested headwater catchment. *Journal of Geophysical Research: Biogeosciences*, *127*, e2022JG006831. https://doi.org/10.1029/2022JG006831

Received 31 JAN 2022
Accepted 2 DEC 2022

Author Contributions:

Conceptualization: Katharina Blaurock, Phil Garthen, Luisa Hopp
Formal analysis: Katharina Blaurock, Phil Garthen, Maria P. da Silva
Funding acquisition: Burkhard Beudert, Benjamin S. Gilfedder, Jan H. Fleckenstein, Stefan Peiffer, Luisa Hopp
Investigation: Katharina Blaurock, Phil Garthen, Maria P. da Silva
Methodology: Katharina Blaurock, Phil Garthen, Maria P. da Silva, Burkhard Beudert, Benjamin S. Gilfedder, Jan H.

1. Introduction

Despite freshwater systems covering less than 3% of the Earth's surface, carbon fluxes from terrestrial into freshwater systems play an important role in the global carbon cycle (Battin et al., 2009; Cole et al., 2007; Raymond et al., 2013). A recent study estimated that 5.1 Pg terrestrial carbon are transported into inland waters every year (Drake et al., 2018). However, there are still many uncertainties regarding the export of carbon from terrestrial systems, which includes particular organic carbon, dissolved inorganic carbon and dissolved organic carbon (DOC). DOC is an important component of dissolved organic matter (DOM), which is a complex mixture of heterogeneous compounds. As carbon is the main element of DOM, DOC is often used as a proxy for DOM

Fleckenstein, Stefan Peiffer, Oliver J. Lechtenfeld, Luisa Hopp
Writing – original draft: Katharina Blaurock
Writing – review & editing: Katharina Blaurock, Phil Garthen, Maria P. da Silva, Burkhard Beudert, Benjamin S. Gilfedder, Jan H. Fleckenstein, Stefan Peiffer, Oliver J. Lechtenfeld, Luisa Hopp

amount (Jaffé et al., 2008; Leenheer & Croué, 2003). DOC also plays an important role in the context of climate change as the largest part of carbon in inland waters (3.9 Pg yr^{-1}) is lost to the atmosphere as the greenhouse gases CO_2 and CH_4 as a result of respiration processes (Drake et al., 2018).

During the last few decades, increases in DOC concentrations in surface waters in the Northern Hemisphere have been observed (Evans et al., 2005; Monteith et al., 2007; Roulet & Moore, 2006), possibly influencing terrestrial carbon storage as a result of leaching (Batjes, 2014; Dixon et al., 1994; Kindler et al., 2011), greenhouse gas emissions (Battin et al., 2009) and drinking water quality (Alarcon-Herrera et al., 1994; Ledesma et al., 2012; Sadiq & Rodriguez, 2004). Several hypotheses have been proposed to explain these increases in DOC in surface waters. The majority of studies suggest the decline in atmospheric sulfur deposition as the main factor (Evans et al., 2006; Hruška et al., 2009; Ledesma et al., 2016; Monteith et al., 2007), whereas other studies suggest alternative explanations such as a decline in nitrogen deposition (Musolff et al., 2016), temperature increase (Weyhenmeyer & Karlsson, 2009), increased iron reduction (Knorr, 2013) and an increase in precipitation (Hongve et al., 2004).

DOC concentrations in discharge from forested catchments in humid, temperate as well as boreal zones positively correlate with the area of wetland soils within these catchments (Laudon et al., 2011; Musolff et al., 2018). Although not all riparian zones are wetlands, many riparian zones are similar to wetlands especially regarding the biogeochemistry of the saturated soils (Vidon, 2017). Riparian zones might also include so-called cryptic wetlands, which are hidden under forest canopy and can strongly contribute to DOC export from catchments (Creed et al., 2003). Indeed, the riparian zone is generally regarded to be of great importance for DOC export due to the accumulation of soil organic matter and the often high groundwater level (Grabs et al., 2012; Inamdar & Mitchell, 2007; Ledesma et al., 2015; Ledesma, Kothawala, et al., 2018; Mei et al., 2014; Musolff et al., 2018; Ploum et al., 2020; Strohmeier et al., 2013). Therefore, hydrological connectivity between the riparian zone and streams has important implications for DOC export (Birkel et al., 2017; Bishop et al., 2004; Blaurock et al., 2021; Broder et al., 2017; Werner et al., 2021). Hydrological connectivity and, therefore, runoff and solute response to precipitation are dependent on the antecedent hydrological conditions in a catchment as well as individual event characteristics (Blaurock et al., 2021; Detty & McGuire, 2010; McGuire & McDonnell, 2010; Penna et al., 2015). Hydrological connectivity influences which parts of the riparian zone contribute to discharge and DOC export. However, the riparian zone is often very heterogeneous, varying in width (Ledesma, Futter, et al., 2018), vegetation (Kuglerová et al., 2014; Park & Kim, 2020), carbon content (Blazejewski et al., 2009), soil composition (Grabs et al., 2012), permeability (Vidon & Hill, 2004) and hydrological connectivity (Ledesma, Futter, et al., 2018; Ploum et al., 2020). It has been shown that surface microtopography in wetland systems can strongly influence hydrological connectivity, internal biogeochemical cycling and runoff generation (Antoine et al., 2009; Frei et al., 2010) as well as the formation of biogeochemical hot spots (Frei et al., 2012).

Several studies have investigated biogeochemical differences in relation to microtopographical heterogeneity (Courtwright & Findlay, 2011; Cresto Aleina et al., 2015; Diamond et al., 2021; Mazzola et al., 2021). Werner et al. (2021) have recently shown that wet depressions contributed strongly to DOC export in the riparian zone of a forested catchment. In a previous study, we used high-frequency, in-stream DOC data to demonstrate that DOC export from the riparian zone of a headwater catchment in the Bavarian Forest National Park (BFNP) is strongly dependent on hydrological connectivity between the riparian zone and the stream (Blaurock et al., 2021). The present study expands this with the aim to identify the source areas of DOC in the same riparian zone. The focus of the present study was on understanding the role of microtopography for DOC mobilization and DOM quality in the stream and riparian zone. In addition to measuring DOC concentrations, we used absorbance and fluorescence spectrometry as well as Fourier transform ion cyclotron resonance mass spectrometry (FT-ICR-MS) to investigate DOM quality in the riparian zone. We linked our observations of DOC concentrations and DOM quality to the local microtopography and hydrological connectivity between the riparian zone and the stream. We hypothesize that groundwater dynamics, DOM quality, and geochemical characteristics differ between locations with and without a pronounced microtopography in the riparian zone. Moreover, we hypothesize that microtopographical depressions (called "ponds" hereafter) influence the amount of DOC exported to the stream during precipitation events and that the contribution of this DOC can subsequently alter stream DOM quality.

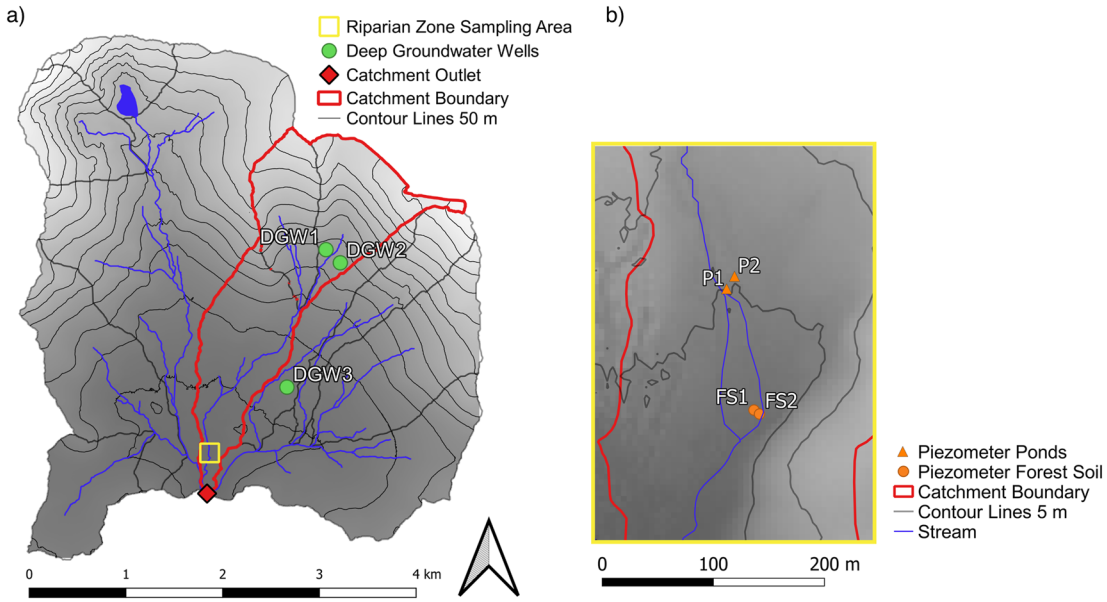

Figure 1. (a) The Hinterer Schachtenbach catchment (outlined in red) as part of the Groβe Ohe catchment. The elevation in this catchment ranges from 771 m a.s.l. (dark gray) to 1,373 m a.s.l. (light gray). Discharge, precipitation, and stream chemistry parameters were measured at the catchment outlet (red diamond). Deep groundwater samples were taken at three wells located at different topographical positions (green dots). Shallow groundwater was sampled in piezometers located in the riparian zone sampling area (yellow square), which is shown in more detail on the right side. (b) The riparian zone sampling area with the locations of the two piezometers located in the forest soil (orange circles) and the two piezometers located in the ponds (orange triangles). The stream splits in two parts, whereas the Western branch is the main stream and the Eastern branch is smaller and of lower discharge. Note that panel "b" does not fully represent the riparian zone sampling area depicted in panel "a". Stream channels were identified using a 5 m resolution digital elevation model (DEM). Both the location of the stream channels and the DEM were provided by the Bavarian State Office for Environment.

2. Materials and Methods

2.1. Study Site

The study was conducted in the Groβe Ohe catchment (19.2 km^2) within the BFNP (243 km^2), located in Southeast Germany. Measurements were conducted in the sub-catchment Hinterer Schachtenbach (3.5 km^2; Figure 1a).

The elevation in this sub-catchment ranges from 771 to 1,355 m a.s.l. with a mean slope of 12°. The geology of the catchment is dominated by biotite granite and cordierite-sillimanite gneiss. The soils are mainly cambisols (66%) together with hydromorphic soils (17%) and podzols (15%). Mean annual precipitation is 1,323 mm and mean annual temperature is 6.5°C (1990–2019). The entire catchment is covered by forest, with Norway spruce (*Picea abies*, 70%) and European beech (*Fagus sylvatica*) as dominant tree species. Large parts of the catchment are in a stage of rejuvenation after bark beetle outbreaks in the mid-1990s (Beudert et al., 2015).

2.2. Collection of Field Data

In order to characterize possible DOC source areas in the riparian zone and gain further insights into their role for DOC export during a precipitation event, we collected field data over the sampling period from May until October 2020. With the goal to identify differences in DOM quality and water chemistry of shallow groundwater, which can be linked to microtopography, we sampled shallow groundwater at two representative locations in the riparian zone: below the typical forest soil and below small ponds (ca. 2–3 m^2, see Figure 4 for an example), which are a common feature of the large flat riparian zone of the catchment. The origin of these ponds is unclear. Those two locations are representative for two typical types of shallow groundwater in the riparian zone, which we assume is important for DOC export in this catchment. To investigate if potential differences between the shallow groundwaters can be traced back to differences in the solid phase, soil samples were taken at the same locations. Although it can be assumed that shallow groundwater is the most important DOC source during events, we took additional samples of deep groundwater to account for its possible influence on event-based DOC export. With the goal to elucidate the influence of the possible DOC source areas on in-stream DOC concentrations and

quality, we investigated chemical in-stream changes during one precipitation event, which was unusually large for the sampling period. In the following, we explain the sampling methods and measurements in detail.

2.2.1. Precipitation and Discharge Data

Precipitation was measured with a resolution of 10 min at a meteorological station at the catchment outlet (770 m a.s.l.) and was provided by the BFNP. Starting in June 2018, the water level was measured every 15 min at the catchment outlet using a pressure transducer (Solinst Canada Ltd., Georgetown, Canada and SEBA Hydrometrie GmbH, Kaufbeuren, Germany). Discharge was measured periodically at the same location with an electromagnetic current meter (FlowSens, SEBA Hydrometrie GmbH, Kaufbeuren, Germany) and via tracer-dilution (TQ-S, Sommer Messtechnik, Koblach, Austria) to establish a rating curve and generate continuous flow data.

2.2.2. Deep Groundwater Sampling

Each of three deep groundwater wells (Figure 1) were sampled in March 2021: DGW1 (969 m a.s.l., 16. 5 m depth), DGW2 (964 m a.s.l., 17.5 m depth) and DGW3 (819 m a.s.l., 10.3 m depth). Monthly long-term DOC concentrations were provided by the BFNP (unpublished data) for the sites DGW1 (2002–2020) and DGW3 (2001–2020) and showed few long-term temporal variations (0–1.26 mg L^{-1} with a mean of 0.34 mg L^{-1} for DGW1 and 0.06–2.15 mg L^{-1} with a mean of 0.57 mg L^{-1} for DGW3). As the DOC concentrations in the samples from March 2021 (0.74 mg L^{-1} for DGW1, 0.67 mg L^{-1} for DGW2 and 0.78 mg L^{-1} for DGW3) were in the range of long-term DOC concentrations (Figure S1 in Supporting Information S1), we assumed that measured absorbance characteristics and water chemistry parameters were representative for the deep groundwater.

2.2.3. Shallow Groundwater Monitoring and Sampling

Two piezometers (*P*1 and *P*2) were installed in two different vegetation-free ponds at a depth of 40 and 84 cm BGL (below ground level), respectively. They were located close to the main stream (ca. 600 m upstream of the catchment outlet) and to a branch-off of the stream (5 m for *P*1 and 17 m for *P*2; Figure 1b) with the pond bottom being higher than the stream level but lower than the surrounding topography. Two piezometers (FS1 and FS2) were installed in the grass-covered, flat forest soil at a depth of 87 and 50 cm BGL, respectively. They were located close (19 m for FS1 and 5 m for FS2) to the small branch of the stream but further away from the main stream (33 and 49 m; Figure 1b). Depth varied due to local differences in soil penetrability. All piezometers were screened over 9 cm starting 8 cm from the tip. The shallow groundwater level (called "water level" hereafter) was measured in FS1, FS2, and *P*1 (but not in *P*2) at a 15 min interval starting in June 2020 using pressure transducers (Solinst Canada Ltd., Georgetown, Canada). The pressure transducers were barometrically corrected and water depth was adjusted to manual measurements of the water level. From 25th of July until 21st of September 2020 and from 8th of October until 30th of October 2020, a time lapse camera took pictures of the pond *P*1 at an interval of 30 min. To test for temporal concentration changes, shallow groundwater was sampled from all four piezometers manually using a bailer approximately every three weeks from May until October 2020 resulting in a total of 11 samples per piezometer. Additionally, the pond water itself was sampled at *P*1 and *P*2 on five dates. Before the shallow groundwater sampling, all water was removed completely from the piezometers and samples were taken from the refilled water. The samples used for molecular analysis (using FT-ICR-MS, see Text S1 in Supporting Information S1) were collected separately: A sample of FS1 and a sample of FS2 were manually collected using clean glass bottles (rinsed with ultrapure water and heated for 4 hr at 400°C) in September 2020, but no samples from *P*1 and *P*2 were collected.

2.2.4. Soil and Pore Water Sampling

The soil profile at FS1 was sampled once by taking six samples using a soil corer over the depth of 5–65 cm in October 2020. Furthermore, one grab sample of the topmost 5 cm at *P*1 was taken in June 2020. Pore water was sampled at *P*1 and *P*2 with a resolution of 2 cm to a depth of 20 cm using peepers filled with deionized water which were left to equilibrate with soil water between 16 and 22 days. As for most parameters and sampling dates, no variation with depth was observed and DOC concentrations as well as DOM quality of the pore water samples were similar to the shallow groundwater sampled with the piezometers (Figure S2 in Supporting Information S1), only shallow groundwater data are shown in this study.

2.2.5. Sampling of a Precipitation Event

During an event from 25th to 27th of September (63 mm), stream water was sampled hourly using a portable water sampler (ISCO Sampler, Teledyne, Thousand Oaks, United States) close to the catchment outlet (red diamond,

Figure 1a) resulting in 47 samples. One sample was taken during baseflow shortly before discharge started to increase in order to compare changes to pre-event conditions. For the molecular analysis, which requires a higher volume of sample, five to six stream samples from the portable water sampler were pooled before filtration (Table S1 in Supporting Information S1). Therefore, the first sample point in the FT-ICR-MS data also includes the very early event flow in addition to pre-event baseflow.

2.3. Laboratory Analysis

2.3.1. Analysis of Water Chemistry Parameters

All water samples were filtered using polycarbonate track etched membrane filters (LABSOLUTE, 0.4 µm) for the samples taken during the precipitation event and polyethersulfone membrane filters (0.45 µm) for all other samples. All samples were stored until further analyses at 4°C in the laboratory (up to 11 days with the exception of the first sampling date where 41 days elapsed before measurement). DOC concentrations of 23 event samples (out of 47), 44 shallow groundwater samples and three deep groundwater samples were analyzed by thermo-catalytic oxidation (TOC-L-Analyzer, Shimadzu, Kyoto, Japan). Samples for cation analysis (47 event samples, 44 shallow groundwater samples, and three deep groundwater samples) were stabilized with 1 vol% 1M HNO_3. Cation concentrations of Al, Ca, Fe, Mg, and Mn were determined using inductively coupled plasma optical emission spectrometry (ICP-OES XL 3200, PerkinElmer, Waltham, United States).

Concentrations of Fe(II) of six shallow groundwater samples were determined photometrically at 512 nm (DR 3800, Hach Lange, Düsseldorf, Germany) after adding phenanthroline (0.5%) to the samples (Tamura et al., 1974). Subsequently, Fe_{tot} was measured by reducing Fe(III) to Fe(II) with ascorbic acid (10%). Fe(III) concentrations were calculated by subtracting Fe(II) from Fe_{tot}. In addition to the laboratory analyses, pH of all water samples was measured in the field on two sampling dates.

2.3.2. Spectroscopic Measurements for the Characterization of DOM Quality

All spectroscopic measurements were conducted at 20°C. Samples were not acidified to avoid the flocculation of DOC and other spectroscopic artifacts. Absorbance measurements of samples (23 out of 47 event samples, 44 shallow groundwater samples and three deep groundwater samples) were performed using UV-Vis spectrophotometry (Cary 100, Varian, Palo Alto, United States), which recorded the absorption spectrum of water samples from 200 to 800 nm with a resolution of 0.5 nm. Blanks were subtracted from the absorbance spectra. Two commonly used absorbance metrics were determined: The ratio between the absorbance at 254 and at 365 nm (A_{254}/A_{365}), which is negatively correlated to the molecular weight of DOC (Dahlén et al., 1996), and the specific UV absorbance defined as the DOC concentration normalized absorbance at 254 nm ($SUVA_{254}$), which is positively correlated to DOC aromaticity (Weishaar et al., 2003). As iron was present mainly as Fe(II), we refrained from correcting the SUVA values for samples with high iron concentrations (Poulin et al., 2014). The spectral slope ratio (S_R) was calculated by dividing the slope in the interval of 275–295 nm by the slope at 350–400 nm. Slopes were determined using linear regression of log-transformed absorption spectra. S_R has been shown to be inversely related to molecular weight (Helms et al., 2008).

Fluorescence parameters in shallow groundwater were measured for eight out of eleven sampling dates, for a total of 32 samples. Prior to analysis, samples were diluted to absorption at 254 nm < 0.3 cm^{-1} to reduce inner-filter effects if necessary. A fluorescence spectrometer (LS-55, PerkinElmer, Waltham, United States) recorded fluorescence Excitation-Emission Matrices in 5 nm steps over an excitation range of 240–450 nm and in 0.5 nm steps over an emission range of 300–600 nm. Blanks were subtracted from the fluorescence spectra. No Raman normalization was conducted, as ratios were used for further analysis instead of the absolute values. The Fluorescence Index was calculated as the ratio between emission at wavelengths of 470 and 520 nm at an excitation wavelength of 370 nm. Higher values are related to a lower aromatic content and greater fraction of microbially derived material and lower values are related to a higher aromatic content, which is typical for DOC of terrestrial origin (Cory & McKnight, 2005; McKnight et al., 2001). The Freshness Index was calculated as the ratio between emission at 380 nm and the emission maxima between 420 and 435 nm at an excitation of 310 nm. The Freshness Index is positively correlated with the contribution of recently produced versus more decomposed DOC (Parlanti et al., 2000). The Humification Index (HIX) was calculated by dividing the emission intensity in the 435–480 nm region by the sum of emission intensities in the 300–345 and 435–480 nm at an excitation of 255 nm (Ohno, 2002). HIX has been shown to range from 0 to 1 with an increasing degree of humification,

aromatic content, and molecular complexity. Fluorescence results of the deep groundwater samples were not included in the analysis as the very low DOC and very low fluorescence values in general may bias the ratios. Absorbance and fluorescence indices have been used in a large number of studies with the goal to gain insights into DOM origin and composition. They were developed partly for very different environments (e.g., the Fluorescence Index on lake samples from Antarctica or the Freshness Index for marine ecosystems). Generally, it remains unclear if these indices can be interpreted in terrestrial ecosystems in the same way as for their original purpose. In this study, we use the indices primarily to highlight qualitative differences between DOC sources and not to characterize DOC itself. In the following, we refer to the calculated absorbance and fluorescence metrics as "DOM quality parameters".

2.3.3. FT-ICR-MS Measurements and Processing

To calculate the probability of the existence of aromatic structures, the modified aromaticity index (AI mod) was used (Koch & Dittmar, 2006, 2016). DOM composition was analyzed based on aggregated DOM molecular descriptors (H/C_{wa}, O/C_{wa}, and AI mod_{wa}) calculated from the intensity-weighted average (wa) of AI mod and elemental ratios (H/C and O/C) of all molecular formulas present in the samples. The detailed description of FT-ICR-MS measurments and processing can be found in Text S1 in Supporting Information S1.

2.3.4. Soil Sample Analysis

Reactive iron was extracted by shaking 200 mg of soil mixed with 20 mL 1M HCl for 24 hr. Subsequently, Fe(II) and Fe_{tot} were measured photometrically as described in 2.3.1. Pedogenic iron oxides were extracted by heating 1 g of soil with 20 ml of 0.3 M sodium citrate ($C_6H_5Na_3O_7$ x 2 H_2O), 5 ml of 1M sodium hydrogen carbonate ($NaHCO_3$) and 0.5 g solid sodium dithionite ($Na_2S_2O_4$) following Mehra and Jackson (1958). The extracts were filtered (0.45 µm) and diluted to 1:10. Fe and Al concentrations were determined using inductively coupled plasma optical emission spectrometry (ICP-OES XL 3200, PerkinElmer, Waltham, United States). C and N content were determined using an elemental analyzer (FlashEA1112, Thermo Fisher Scientific, Waltham, USA).

2.4. Data Analysis

2.4.1. Analysis of Differences in Groundwater Dynamics

As a measure of event flow, the 0.9 quantile ($Q_{0.9}$) of all discharge values during the sampling period was calculated. For all data points with discharge values above $Q_{0.9}$, the mean shallow groundwater level for each location was calculated, representing the mean groundwater level during event flow. Additionally, we used the metric t_R, which was defined as the time (in minutes) needed for the water level to recede by 2 cm from the water level maximum during an event. t_R was calculated for 15 events, for which water level data was available and which resulted in a visible water level peak at all three locations (FS1, FS2, *P*1). The presented t_R values refer to the mean of the 15 analyzed events ± standard deviation.

2.4.2. Statistical Analysis of Potential DOC Source Areas

The sampled locations FS1, FS2, *P*1, *P*2, and DGW were interpreted as representing different source areas of DOC. We call these source areas also "end-members" hereafter, following the terminology used in hydrograph separation studies. However, our intention was not to perform a full hydrograph separation, but to focus on the role of different source areas in the riparian zone for stream chemistry during events. Moreover, our sampled end-members exhibited slightly varying concentrations over time for some of the parameters and were thus not strictly consistent with the assumptions made in an end-member mixing analysis (Christophersen et al., 1990). Therefore, instead of using the end-members to quantify their contribution to streamflow, we investigated the qualitative differences between the end-members and their qualitative influence on the composition of the stream water. The sampled locations were grouped according to their physiographic characteristics: (a) FS1 and FS2 as representatives for sites with a typical forest soil (called FS, hereafter), (b) *P*1 and *P*2 as representatives for sites with ponds (called *P*, hereafter) and (c) DGW1, DGW2, and DGW3 as representatives for the deep groundwater (called DGW, hereafter). A cluster analysis was performed to verify the similarity of the grouped end-members. $SUVA_{254}$ and concentrations of DOC, Fe, Al, Mn, Mg, and Ca were included in the cluster analysis. The other parameters were excluded due to the low concentrations in the groundwater samples. All samples, for which all selected parameters were available, were included ($n_{FS1} = 10$, $n_{FS2} = 11$, $n_{P1} = 10$, $n_{P2} = 11$, $n_{DGW1} = 1$, $n_{DGW2} = 1$, $n_{DGW3} = 1$). All data were normalized prior to analysis by centering and scaling the data to a mean of 0 and a

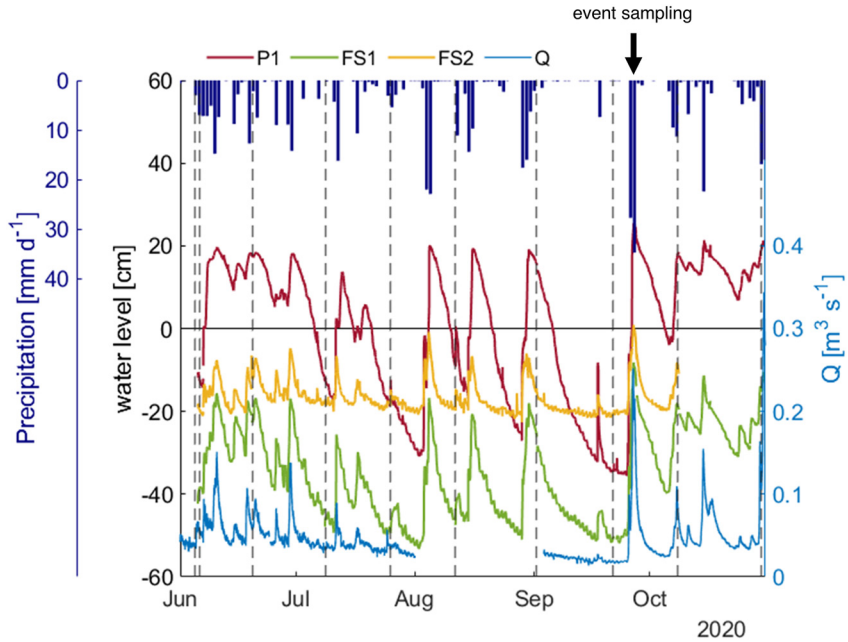

Figure 2. Water levels below ground [cm] during the sampling period from June to October 2020 at the locations FS1, FS2, *P*1, precipitation [mm d^{-1}] and discharge (Q [m^3 s^{-1}]) at the catchment outlet. Positive water level values of *P*1 indicate that the pond *P*1 was filled with water, that is, 0 cm refers to the pond bottom (black horizontal line). The highest water level of *P*1 corresponds to the point of spillover. Due to a technical failure, the water level values for FS2 are only available until the beginning of October and there is a data gap for discharge during August. Dashed lines indicate the dates when shallow groundwater was sampled from the piezometers. As the first sampling date was in May, it is not visible in this figure. The sampled event took place from 25th to 27th of September (black arrow).

standard deviation of 1. Following the cluster analysis, a Wilcoxon ranksum test for all analyzed parameters (DOC, $SUVA_{254}$, A_{254}/A_{365}, Freshness Index, Fluorescence Index, HIX, S_R, Fe, Al, Mn, Mg, Ca) was performed in order to test the similarity between the sampled end-members *P* and FS (but not DGW). To investigate chemical in-stream changes, a linear regression between the parameters and stream discharge during the precipitation event was performed. All statistical analyses were performed using MATLAB (MATLAB R2019b).

3. Results

3.1. Meteorological Conditions and Hydrological Dynamics in the Riparian Zone

The year of our investigation showed some deviations from the long-term hydro-meteorological conditions in the catchment (reference period 1990–2019). The total annual precipitation in 2020 was 1,134 mm, which was lower than the long-term average of 1,323 mm. The sampling period (June–October) was slightly drier in 2020 (523 mm) than the long-term mean precipitation of the reference period (541 mm). The annual mean temperature for 2020 was 1.1°C higher than the long-term average while the sampling period was 0.7°C warmer than the long-term mean temperature of the same months. The sampled event at the end of September was an unusually large event (63 mm of total precipitation) for the sampling period.

The water levels in the riparian zone were highly dynamic during the entire sampling period and responded strongly and quickly to precipitation (Figure 2).

The largest changes in water level were observed at *P*1, varying between 36 cm BGL and 26 cm above ground level (AGL), resulting in a difference of 62 cm. The water level did not increase to levels higher than 26 cm AGL, even with further increasing discharge. The changes in water level at the locations in the forest soil were smaller. At FS1, the water level was lowest and fluctuated between 53 and 8 cm BGL, resulting in a difference of 45 cm. At FS2, the water level varied between 23 cm BGL and 1 cm AGL, resulting in a difference of 24 cm. The water levels started to decrease faster at FS1 and FS2 (t_R of 587 ± 230 and 520 ± 250 min, respectively) after reaching the maximum in contrast to *P*1, where water levels stayed high during a longer period (t_R of 1,504 ± 1,130 min).

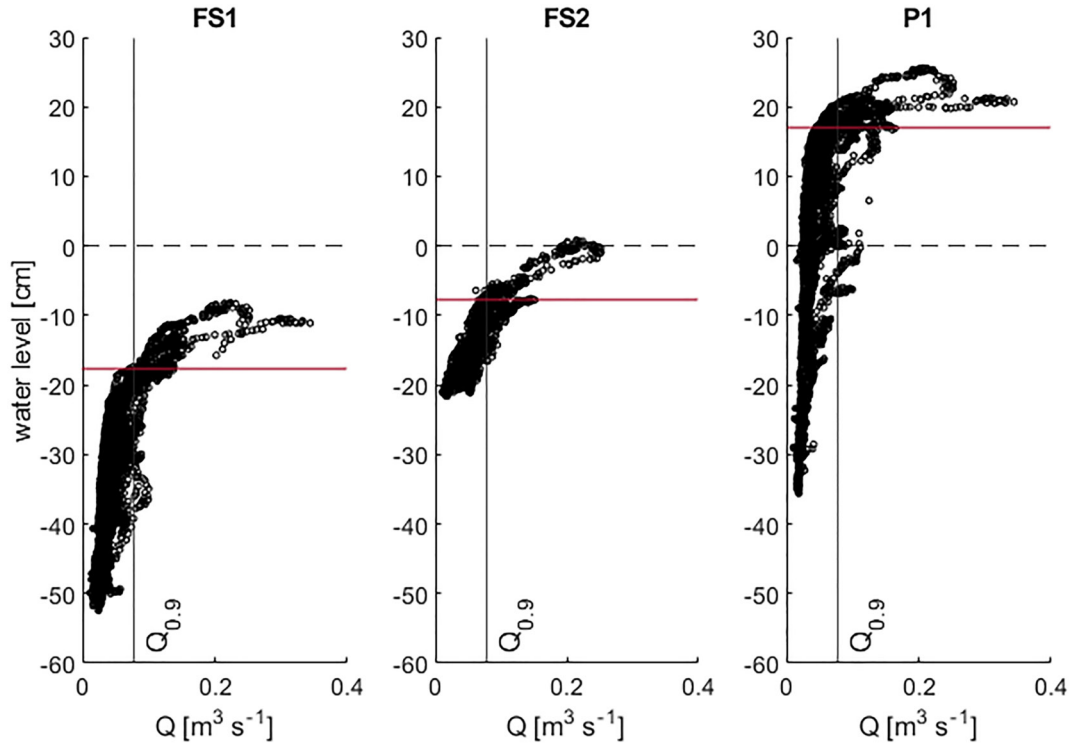

Figure 3. The relationship between the water level [cm] in the piezometers at the locations FS1, FS2, and *P*1 and stream discharge Q [m^3 s^{-1}] during the complete sampling period. The dots represent 15 min time steps. The horizontal black dashed line indicates the soil surface, where the piezometer emerge from the soil. The vertical black line indicates the 0.9 quantile ($Q_{0.9}$) for all discharge values. The horizontal red line indicates the mean water level for all data points with discharge values above the $Q_{0.9}$.

At all three sites, a nonlinear relationship between water level and discharge was visible, showing a stronger water level increase at lower discharge values and a lower water level increase at higher discharge values (Figure 3). The mean water level for discharge values above $Q_{0.9}$, varied between the locations: For FS1, it was located at 17.7 cm BGL, for FS2, it was located at 7.8 cm BGL and for *P*1, it was located at 16.9 cm AGL.

The filling and emptying of the ponds could also be monitored using the time lapse camera. No images were available for the event in September, which we will discuss in detail in Section 3.3. As an example of the water level reaction in the ponds (Figure 4) we, therefore, show here the water levels in *P*1, FS1, and FS2 and images of the temporal changes at *P*1 during an event at the beginning of August.

The water level at *P*1 typically started to rise one to 2 hr after the beginning of a precipitation event. Large events led to a filling of the pond. During most events, the water in the pond continued to rise after the end of the precipitation event, reaching the maximum several hours later. When the water level in the ponds reached the level of the surrounding ground surface, the ponds would spill and connect in a cascading manner with each other and eventually to the stream, thereby creating short periods of overland flow toward the stream. If no precipitation event followed, the water level decreased slowly over the course of days (Figure 4).

3.2. Characterization of DOC Source Areas

The cluster analysis confirmed the selection of the end-members FS, *P*, and DGW (Figure S3 in Supporting Information S1). Most parameters determined in the aqueous phase showed clear differences between the end-members FS, *P*, and DGW. DOC, SUVA, Freshness Index, Fluorescence Index, HIX, Al, Mn, Ca, and Mg showed significant differences between the shallow groundwater end-members FS and *P* ($p < 0.05$; Figure 5). In contrast, the parameters A_{254}/A_{365}, S_R, and Fe did not show significant differences between FS and *P* ($p > 0.05$; Figure 5). DGW showed the lowest concentrations of DOC, SUVA, Al, Fe, Mg, and Mn and an intermediate concentration of Ca. Site FS was characterized by lower DOC and Al concentrations than *P* and higher Ca, Mg,

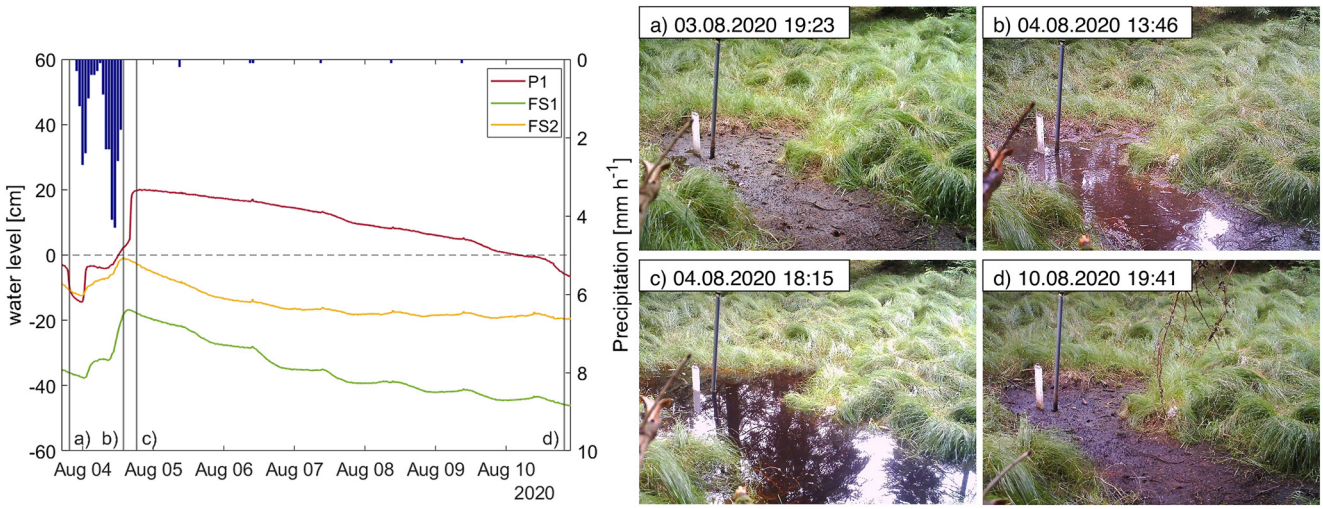

Figure 4. Left side: Hourly precipitation and water levels in the piezometers at the locations FS1, FS2, and *P*1 during the event of 4 August 2020. Values above the horizontal dashed line indicate that the groundwater is rising above the surface and filling the pond. Right side: Pictures taken at *P*1 with a time lapse camera (a) before the event, (b) during the rising limb of the hydrograph, (c) at the maximum water level, and (d) at the lowest water level before the start of the next event. The times correspond to the vertical gray lines in the left side figure.

and Mn concentrations. On average, 88.3% ± 9.7% of the dissolved Fe at site FS was present as Fe(II). The Freshness Index and Fluorescence Index were higher at site FS than at site *P*, whereas HIX and SUVA were lower at site FS than at site *P*. On average, 91.6% ± 5.4% of the dissolved Fe at site *P* was present as Fe(II). Site FS had a higher pH (mean value of 6.2) than site *P* (mean value of 4.8). In the solid phase, site FS had higher contents of reactive iron and of pedogenic iron, but a lower content of pedogenic aluminum and of total carbon than site *P* (Tables S2 and S3 in Supporting Information S1).

Analyses of DOC concentrations, absorbance parameters and fluorescence parameters in the pond water itself (data not shown) revealed no significant difference to the shallow groundwater at site *P* for DOC concentrations, A_{254}/A_{365}, Freshness Index and HIX (Wilcoxon ranksum, $p > 0.05$) but a significant difference for the Fluorescence Index and S_R (Wilcoxon ranksum, $p < 0.05$).

3.3. Hydrochemical Response of the Stream Water During the Analyzed Event

There were clear changes in various parameters in the stream water over the course of the investigated event. DOC, SUVA, Al, Fe, and Mn showed a significant positive relationship with discharge (Figure 6; $p < 0.05$; $R^2_{DOC} = 0.75$, $R^2_{SUVA} = 0.52$, $R^2_{Al} = 0.75$, $R^2_{Fe} = 0.81$, $R^2_{Mn} = 0.91$). Mg showed a significant negative relationship with discharge ($p < 0.05$; $R^2_{Mg} = 0.16$). Ca, Fluorescence Index, Freshness Index, A_{254}/A_{365}, HIX and S_R showed no relationship with discharge ($p > 0.05$; $R^2_{Ca} = 0.02$, $R^2_{Fluorescence} = 0.05$, $R^2_{Freshness} = 0.04$, $R^2_{A254/A365} = 0.12$, $R^2_{HIX} = 0.17$, $R^2_{SR} = 0.01$). For DOC, SUVA, HIX, Al, Fe, Mn, and Mg, there was a significant difference ($p < 0.05$) between the in-stream values during the first half of the event, when the ponds were empty, and the second half of the event, when they were full (Figure 7). For DOC, SUVA, HIX, Al, and Mg the values clearly changed into the direction of the values found at *P* (red line in Figure 6). Mn and Fe are generally higher at both FS and *P* than in the stream. For the molecular data, no comparison with *P* was possible. However, a clear change in H/C_{wa}, O/C_{wa}, and AI mod_{wa} was visible over the course of the event. When the ponds were full, all molecular parameters deviated from the values found at FS as H/C_{wa} decreased, whereas O/C_{wa} and AI mod_{wa} increased.

4. Discussion

4.1. Hydrological Dynamics in the Riparian Zone

The sampling period was characterized by declining discharge values with only a few large precipitation events. However, we saw a highly dynamic shallow water level. Generally, a high level of saturation in the riparian zone needs to be reached to establish a significant degree of hydrological connectivity along shallow subsurface and

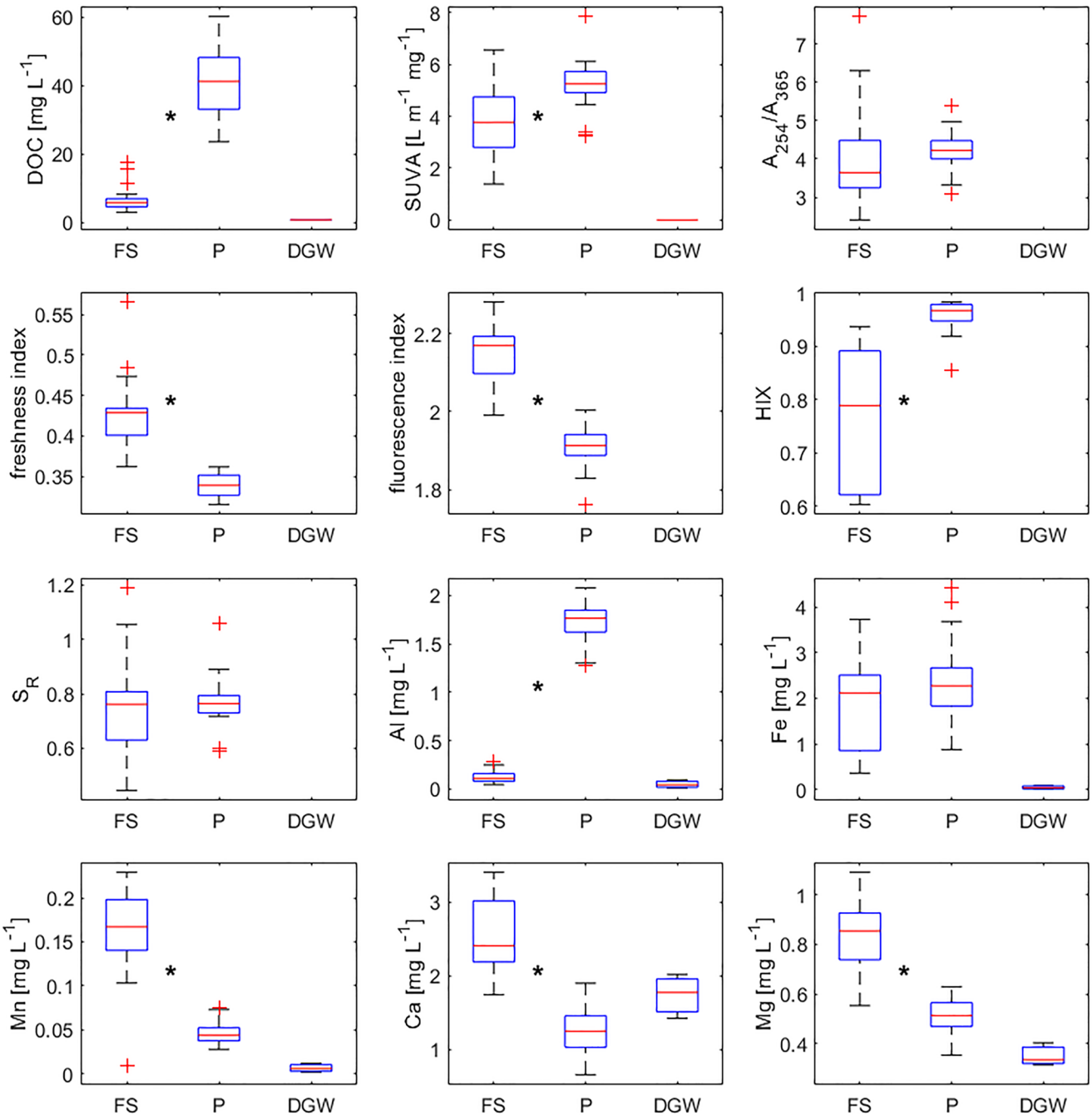

Figure 5. Water chemistry and dissolved organic matter (DOM) quality parameters of the piezometers located in the forest soil (FS), the ponds (*P*), and deep groundwater (DGW). Some parameters do not include DGW data because measured values were too low to be reliable (A_{254}/A_{365}, Freshness Index, Fluorescence Index, HIX, S_R). The bottom and top of each box indicate the 25th and 75th percentiles, respectively. The red line in the middle of each box is the sample median. The red crosses represent outliers and the whiskers extend to the most extreme data points not considered outliers. Asterisks indicate a significant difference ($p < 0.05$, Wilcoxon ranksum test) between FS and *P*.

surficial flow paths to the stream (Blaurock et al., 2021; Ledesma, Futter, et al., 2018; Ploum et al., 2020). At all sites, we observed the characteristic nonlinear relationship between discharge and groundwater level often found in riparian zones (Frei et al., 2010; Ledesma, Futter, et al., 2018; Seibert et al., 2009), which is commonly attributed to a nonlinear increase of the soil transmissivity toward the soil surface. At site FS, the rising water level would lead to the saturation of upper soil layers and a subsequent lateral movement of water through the soil, whereas at site *P* the water level would often rise above the surface. Following a water level rise, the ponds were

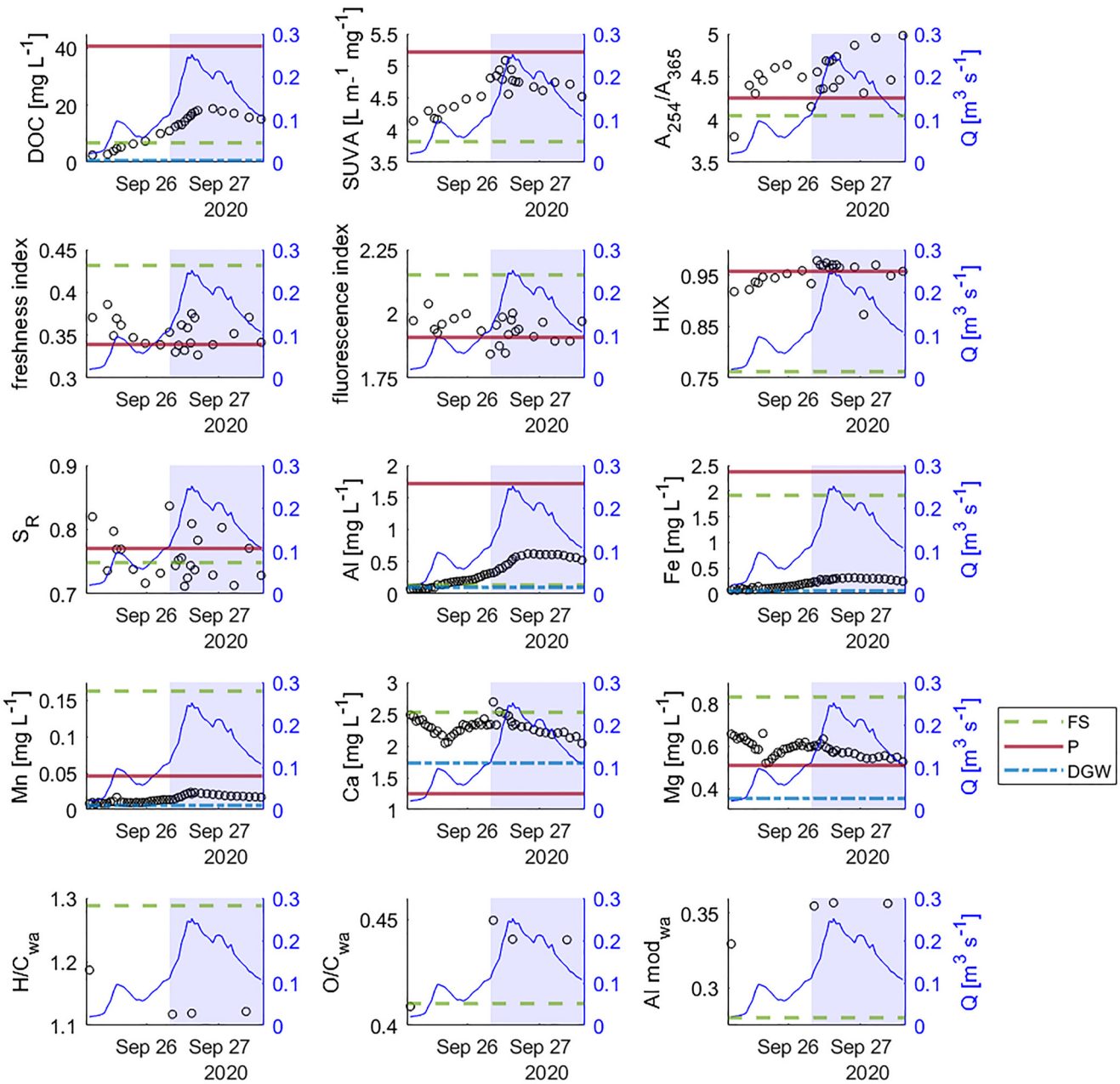

Figure 6. Discharge (blue line) and changes of the hydrochemical and dissolved organic matter (DOM) quality parameters (black circles) of the stream during the event in September 2020 in comparison to the mean concentration of the values found in the piezometers located in the forest soil (green dashed line) and the ponds (red line) as well as the values of the deep groundwater (blue dashed line). The blue shaded area corresponds to the time, during which the ponds were filled with water. The first dot in all panels except for the molecular data represents pre-event conditions. For the molecular data (last row), the dots represent the collection time of the first of the pooled samples (Table S1 in Supporting Information S1).

connected to the stream via overland flow as has been observed in other catchments (Fitzgerald et al., 2003; Frei et al., 2010; Werner et al., 2021). The continuous increase of the water level at site *P* even several hours after the end of precipitation events indicates a time-delayed contribution of water components originating further away from the ponds. Moreover, t_R values showed that the water at site *P* recedes more slowly than at site FS, keeping the upper soil layers wet for a longer time. In summary, the differences in water level dynamics between the locations with and without ponds highlight the structural heterogeneity of the riparian zone, which can strongly influence flow pathways and source waters (Lessels et al., 2016).

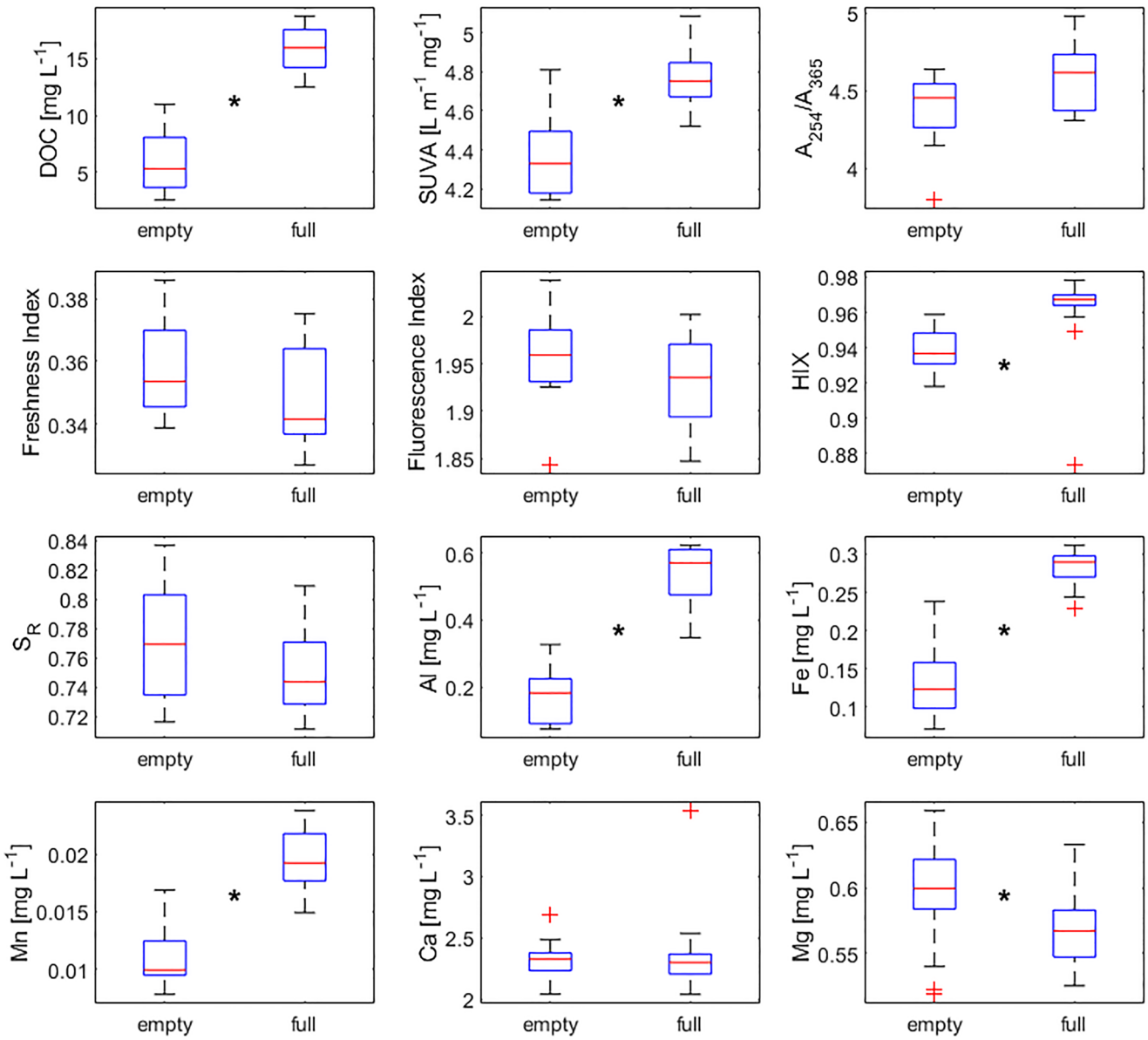

Figure 7. Stream water chemistry and dissolved organic matter (DOM) quality parameters during the event sampled in September 2020 while the ponds were not yet filled with water (empty; unshaded area in Figure 6) and while the ponds were filled with water (full; shaded area in Figure 6). The bottom and top of each box are the 25th and 75th percentiles, respectively. The red line in the middle of each box is the sample median. The red crosses represent outliers and the whiskers extend to the most extreme data points not considered outliers. Asterisks indicate a significant difference ($p < 0.05$, Wilcoxon ranksum test) between empty and full conditions. Molecular data was not included due to the low sampling size.

4.2. Spatial Differences in DOM Quality of Shallow Groundwaters in the Riparian Zone

Pronounced spatial differences in DOC concentrations, DOM quality, and geochemistry were observed between the shallow groundwaters of sites FS and *P* despite the sampling locations being in close proximity to each other relative to catchment size. DOC concentrations in the shallow groundwater exceeded the concentrations found in the stream during baseflow and precipitation events investigated in previous studies (Blaurock et al., 2021; Da Silva et al., 2021). The convergence of DOC-rich subsurface flow pathways (Ploum et al., 2021) or the accumulation of DOC-rich surface water (Scheliga et al., 2019) could have led to the higher DOC concentrations in the topographic depressions at site *P*. Moreover, the large oscillations of the water table at site *P* could indicate a larger dominant carbon source layer and a more frequent activation of it (Ledesma et al., 2015; Ledesma, Futter, et al., 2018). A larger dominant source layer would indicate a larger potential DOC pool. Another reason for the

higher DOC concentrations at site *P* could be a reduced DOC mobility at site FS that exhibited a lower carbon content in the solid phase than site *P*. In subsoil horizons with low carbon content DOC may bind strongly to mineral surfaces, thereby decreasing the mobility of DOC (Kalbitz et al., 2000).

All DOM quality parameters except A_{254}/A_{365} and S_R revealed differences between site FS and site *P*. These differences in DOM quality parameters indicate that the DOM at site *P* is derived from a source that has a different DOM composition than at site FS. Higher SUVA, higher HIX, and lower Fluorescence Index values all indicate a higher DOC aromaticity at site *P* than at site FS (Huguet et al., 2009; McKnight et al., 2001; Weishaar et al., 2003). DOC derived from wetlands or the riparian zone has been described in the literature to be generally more aromatic than DOC derived from other sources (Ågren et al., 2008; Kothawala et al., 2015; Ledesma, Kothawala, et al., 2018; Pisani et al., 2020). As site *P* is more wetland-like than FS due to the regular rewetting, slow drying and the high soil carbon content, a higher aromaticity at site *P* is in line with studies that have found a high aromaticity of DOC in wetlands. Werner et al. (2021) also found that wet areas were characterized by higher DOC concentrations and higher aromaticity than less wet areas. Creed et al. (2003) demonstrated that topographic depressions in forested ecosystems are often hidden wetlands, which contribute strongly to DOC export. Studies have shown that the DOC in upper soil layers is characterized by a higher aromatic content and higher molecular weight than in deeper soil layers (Bausenwein et al., 2008; Corvasce et al., 2006). Upper soil layers also exhibit higher decomposition rates due to the availability of oxygen, nutrients, and higher microbial activity (Fontaine et al., 2007), which leads to the accumulation of aromatic organic matter (Marschner & Kalbitz, 2003). The wet-dry cycles in the ponds are likely to result in a site with high microbiological activity, facilitating DOC production via decomposition of the organic substrate (Borken & Matzner, 2009; Marschner & Kalbitz, 2003). This would explain the occurrence of higher DOC concentrations and more aromatic DOC at site *P* than at site FS.

A second explanation for the distinct DOC characteristics could be the convergence of different flow paths. The delayed increase of the water level following precipitation during some events at site *P* could indicate the connection of flow paths and potentially also DOC sources that are located further away, for example, in the marginal zones of the riparian zone. However, the establishment of hydrological connectivity in the riparian zone and adjacent areas would probably only be linked to large precipitation events or extended wet periods, for example, during snowmelt. One could also argue that differences in DOM quality parameters are a consequence of the source material rather than differences in flow paths or wet-dry cycles. Such differences could be a result of differences in vegetation (Mastný et al., 2018; Spencer et al., 2008). In this study, however, an effect of vegetation on DOM quality is unlikely, as vegetation did not differ among the sampled study sites.

The results highlight that spatial differences in DOM composition can be found not only between forested and wetland catchments (Ågren et al., 2008; Broder et al., 2017; Kothawala et al., 2015) or between riparian zones and upslope soils (Ledesma, Kothawala, et al., 2018), but also at a much smaller scale in the riparian zone itself (Werner et al., 2021). Although there was essentially no significant difference between shallow groundwater and pore water (Figure S2 in Supporting Information S1), vertical heterogeneity in the soils could also play a role in influencing DOM quality at the two sampling sites. However, based on our results we argue that the hydrological differences due to the microtopography are one likely explanation for the observed differences in DOC concentrations and DOM quality. Our findings confirm that local hydrological conditions affect DOC chemistry in the riparian zone (Findlay et al., 2001; Grabs et al., 2012; Ledesma, Kothawala, et al., 2018).

4.3. The Importance of the Ponds for DOC Mobilization During a Precipitation Event

4.3.1. Changes of In-Stream DOM Quality Parameters During a Precipitation Event

Several studies have shown that events contribute substantially to the annual DOC export from catchments (Raymond & Saiers, 2010; Raymond et al., 2016). Large events are known to lead to a larger DOC export as a result of increasing discharge and increasing DOC concentrations (Dawson et al., 2008; Kawasaki et al., 2005; McDowell & Likens, 1988). However, the DOC sources that contribute to DOC export during events depend on catchment and event characteristics. The riparian zone is often a major source for DOC export as the soils are typically DOC rich and hydrological connectivity facilitates DOC export to the stream.

The study design did not allow us to quantify the contribution of the ponds to stream discharge or carbon fluxes as detailed measurements of surface and subsurface fluxes would have been necessary. The contribution of the ponds is also likely to vary with changing antecedent wetness and precipitation. However, our data suggest that

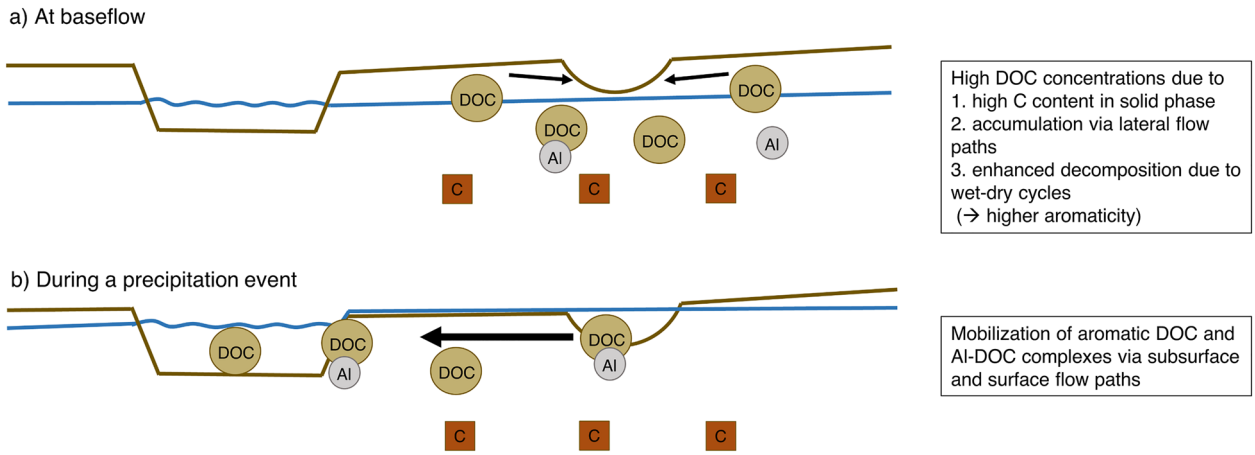

Figure 8. Mechanisms of dissolved organic carbon (DOC) supply in the ponds and its mobilization toward the stream during (a) baseflow and (b) a precipitation event.

the ponds we observed in the riparian zone during wet conditions and the shallow groundwater below could be an important DOC source during precipitation events. During the precipitation event in September 2020, in-stream DOC concentrations increased to over 18 mg L^{-1}, thereby significantly exceeding the shallow groundwater concentrations below the forest soil. This indicated that another source contributed to the in-stream DOC increase during the event. We argue that the shallow groundwater below the ponds, characterized by considerably higher DOC concentrations, probably contributed to event-driven DOC export. As the water level increased at the pond site during the event, DOC-rich water was transported through upper soil layers, which are typically characterized by a higher hydraulic conductivity (Jacks & Norrström, 2004). The water could therefore rapidly transport DOC via subsurface flow toward the stream, possibly exporting even more DOC by passing through the DOC-rich upper soil layer. The formation of cascading sequences of ponds could lead to an even faster transport of the DOC rich water to the stream via overland flow (Figure 8), which could enhance the contribution of the shallow groundwater at site *P* to stream discharge. This is supported by the fact that several stream DOM quality parameters showed a clear trend toward the values found below the ponds. Whereas $A_{254}/A_{365,}$ the Freshness Index, the Fluorescence Index, and S_R did not show a clear trend, possibly due to a low sensitivity to compositional changes during storm runoff (Nguyen et al., 2010, 2013), SUVA increased with discharge as shown in other studies (Fellman et al., 2009; Hood et al., 2006; Vidon et al., 2008) and, at peak discharge, reached almost the same values as found at site *P*. HIX values also significantly increased toward the values found at site *P* during the time, when the ponds were full. Earlier studies have also observed an increase of HIX during precipitation events, which the authors attributed to the increased soil leaching and input of allochthonous organic matter (Nguyen et al., 2010, 2013; Xu et al., 2016).

The additional information on molecular DOC composition provided by FT-ICR-MS data showed that H/C_{wa}, O/C_{wa}, and AI mod_{wa} during the precipitation event deviated from the values found in the shallow groundwater below the forest soil. All pre-event molecular signatures (H/C_{wa}= 1.19, O/C_{wa}= 0.41, AI mod_{wa} = 0.33) were similar to values found in water of a spring close to the stream in an earlier study (H/C_{wa}= 1.18, O/C_{wa}= 0.43, AI mod_{wa} = 0.31; Da Silva et al., 2021). This DOC pool was characterized by aliphatic-like, saturated compounds. The changes in the molecular signatures found during the course of the event indicate that another source contributed to DOC export into the stream. The decrease in H/C_{wa} values pointed to an increase in the unsaturation of compounds. Wagner et al. (2019) also observed decreasing in-stream H/C_{wa} during a precipitation event in a forested catchment and attributed this finding to the export of lignin degradation products and tannins. The proxies for aromaticity calculated from absorption (SUVA) and mass spectrometry data (AI mod_{wa}) are in agreement and indicate an increase in aromaticity over the course of the event. Werner et al. (2021) concluded in their study that the aromatic, H-poor, O-rich DOC that they identified in the stream during an event originated from wet areas. These wet areas were responsible for a large part of DOC export during the event mainly via overland flow. Their findings are in line with our observations that the ponds are contributing to streamflow during precipitation events and that they are exporting aromatic DOC. As similar ponds are located downstream of the investigated area, it is likely that DOC with similar characteristics gets transported into the stream at several input points over the entire reach to the outlet. Possible in-stream processes (Bernal et al., 2019; Lupon et al., 2019) probably play

a minor role for DOC export and quality at the catchment outlet due to (a) the short in-stream residence time between site *P* and the catchment outlet, and (b) input from several ponds along the reach.

4.3.2. Changes of the Stream Water Chemistry During a Precipitation Event

The unclear pattern in Ca and Mg concentrations during the event cannot be used to explain the contribution of potential DOC sources. The increase of Mn concentrations during the precipitation event can be linked to the high Mn concentrations in the upper soil layers below spruce forest as observed in a neighboring catchment (Schwarze & Beudert, 2009). As DOC concentrations were increasing concomitantly with Fe and Al concentrations during the precipitation event, it is likely that DOC, Fe, and Al export were coupled. This observation is consistent with previous studies that observed coupled DOC and Fe concentrations (Bol et al., 2015; Curtinrich et al., 2021; Karlsson & Persson, 2012; Knorr, 2013; Peiffer et al., 1999). The rising water table during events could result in reducing conditions, inducing the release of Fe(II) and DOC via reductive dissolution (Curtinrich et al., 2021; Knorr, 2013; Nieminen et al., 2015; Selle et al., 2019). Subsequently, Fe(II) and DOC could be transported as complexes to the stream. This process could also explain the export of aromatic DOC, which preferentially adsorbs to Fe (Adhikari & Yang, 2015; Grybos et al., 2009; Pan et al., 2016; Riedel et al., 2012). In-stream Fe concentrations clearly increase with discharge and there is a significant difference between the earlier event concentrations, when the ponds were empty, and the later event concentrations, when the ponds were full. However, FS and *P* are both characterized by high Fe concentrations. Therefore, the increase in in-stream concentrations during the event cannot be seen as a sign of an increased contribution of site *P*. Nevertheless, the processes discussed are likely to play a role in DOC mobilization.

In contrast to Fe, Al concentrations are much higher at site *P* than at site FS. Al has also been shown to build complexes with organic matter and therefore it is exported concomitantly without the need for a redox transition (Cory et al., 2007; Palmer et al., 2005; Pellerin et al., 2002; Vogt & Muniz, 1997). The high concentrations likely are a result of the higher Al concentrations in the solid phase at site *P* as well as a result of the increased solubility of Al at low pH (Pellerin et al., 2002). As in-stream Al concentrations during the precipitation event clearly exceeded the concentrations found at site FS and were approaching the concentrations found at site *P*, it is likely that site *P* contributed to the Al increase during the event, as shown in Figure 7. We argue that the concomitant increase of Al and DOC concentrations in the stream indicates the mobilization of Al complexed by DOC from site *P* and, thus, supports the importance of the ponds as source areas for in-stream DOC.

4.4. The Relevance of Riparian Microtopography for Catchment-Scale DOC Export

At our study site, the origin of the microtopographic depressions is unknown. However, microtopographic depressions are a common feature in many catchments worldwide and can often be found in wetlands (Diamond et al., 2021; Nungesser, 2003). Moreover, they can occur after windthrow of trees, resulting in a pit and mound microrelief (Bormann et al., 1995; Ulanova, 2000) or be caused by anthropogenic disturbances, for example, mining activities (Gilland & McCarthy, 2014), the use of heavy machinery in forests during timber harvest (Laudon et al., 2016), exploration activities (Stevenson et al., 2019) or peat extraction from wetlands (Zajac et al., 2018). Also wildfires (Benscoter et al., 2015) or flooding (Stoeckel & Miller-Goodman, 2001) may cause microtopography.

Many studies have shown that microtopography does influence soil properties, soil moisture, and soil biochemical processes (Bormann et al., 1995; Clinton & Baker, 2000; Kooch et al., 2014; Stoeckel & Miller-Goodman, 2001). Moreover, microtopography can have an impact on nutrient availability and dynamics (Minick et al., 2019; Moser et al., 2009; Rogers et al., 2021) and influence the formation of biogeochemical hot spots as a result of complex water flow patterns (Frei et al., 2012).

In this study, we were able to demonstrate that microtopographic depressions could act as hot spots for DOC export as a result of the favorable conditions for DOC accumulation and subsequent transport to the stream. Our finding underpins recent observations demonstrating DOC export is often linked to specific source areas in the riparian zone, which contribute disproportionally to DOC export. Such areas can be narrow soil layers (Ledesma, Futter, et al., 2018) or topographical depressions that determine where water accumulates in the catchment (Ploum et al., 2021; Werner et al., 2021). Ploum et al. (2021) presented the concept of discrete riparian inflow points consisting of topographic depressions that are consistently wetter than the surrounding areas. As a consequence, hydrological pathways are developing that are subsequently enhancing DOC export. Werner et al. (2021) recently

found that microtopographic depressions, which made up 15% of the studied riparian area, were responsible for 1.5 times the DOC export of the remaining 85% of the area. These results point to a disproportional contribution of microtopographic depressions of the riparian zone to DOC export in comparison to their limited area extent.

Hence, microtopographical depressions in riparian zones appear to act as potential hot spots for catchment-scale DOC export. Since they are a very common feature in the riparian zone of many catchments, they may have a much larger influence on in-stream water quality than previously assumed.

5. Conclusions

Our observations show that there are substantial small-scale differences of DOM quality in the riparian zone of our study site. Following precipitation events, hydrological connectivity leads to the export of aromatic DOC and Fe- and Al-DOC complexes into the stream. The in-stream changes of DOC concentrations, DOM quality parameters as well as water chemistry parameters suggest that microtopographic depressions are important sources of DOC that could be rapidly delivered to the stream via overland flow once a threshold water level is reached. These results show that microtopographical structures can be an important DOC source. Moreover, they can alter in-stream DOM quality during events. As a result of climate change, prolonged drought periods and more extreme rain events are to be expected in temperate ecoregions. Longer drought periods would probably reduce the importance of the ponds in terms of exported DOC quantity. However, stronger contrasts in hydrological connectivity and water level dynamics could have an impact on the DOC processing in the upper soil layers, which would lead to more pronounced small-scale spatial differences in DOM quality of the shallow groundwater. These differences could then possibly be seen in the stream during events and influence the further processing of DOC. In summary, we show that the strong interplay between biogeochemical and hydrological processes influences DOC mobilization and processing at small scales in the riparian zone of a headwater catchment. As headwater catchments make up an important part of the global stream length (Downing, 2012), they have the potential to influence large downstream areas (Gomi et al., 2002; Wohl, 2017). Therefore, changes in DOC concentrations or DOM quality in the riparian zone of headwater catchments could also affect DOC export, drinking water quality, or greenhouse gas emissions of downstream river reaches.

Data Availability Statement

The data set used in this study is available at Figshare via https://doi.org/10.6084/m9.figshare.19086455. The original FT-ICR-MS data can be found at https://doi.org/10.48758/ufz.12908.

Acknowledgments
This research has been funded by the Rudolf and Helene Glaser Foundation, as part of the project "Influence of natural factors on concentration, quality and impact of DOC in the BFNP" (Project No. T0083\30771\2017\kg). The authors would like to thank the BFNP administration, for providing physiographic and meteorological data, and the BFNP staff, for their helpful assistance with the installation and maintenance of the field equipment. The authors are also thankful for the personal and technical support obtained through the project "AquaKlif-Influence of multiple stressors on watercourses in climate change" of the Bavarian Climate Research Network BayKlif. The authors acknowledge the European Regional Development Funds (EFRE-Europe funds Saxony) and the Helmholtz Association for supporting the analytical facilities of the ProVIS Center for Chemical Microscopy within the Helmholtz Center for Environmental Research Leipzig. The authors thank Jan Kaesler and Kai Franze for their assistance during FT-ICR-MS measurements and software development. Open Access funding enabled and organized by Projekt DEAL.

References

Adhikari, D., & Yang, Y. (2015). Selective stabilization of aliphatic organic carbon by iron oxide. *Scientific Reports*, *5*(1), 11214. https://doi.org/10.1038/srep11214

Ågren, A. M., Buffam, I., Berggren, M., Bishop, K. H., Jansson, M., & Laudon, H. (2008). Dissolved organic carbon characteristics in boreal streams in a forest-wetland gradient during the transition between winter and summer. *Journal of Geophysical Research*, *113*(G3), G03003. https://doi.org/10.1029/2007JG000674

Alarcon-Herrera, M. T., Bewtra, J. K., & Biswas, N. (1994). Seasonal variations in humic substances and their reduction through water treatment processes. *Canadian Journal of Civil Engineering*, *21*(2), 173–179. https://doi.org/10.1139/l94-020

Antoine, M., Javaux, M., & Bielders, C. (2009). What indicators can capture runoff-relevant connectivity properties of the micro-topography at the plot scale? *Advances in Water Resources*, *32*(8), 1297–1310. https://doi.org/10.1016/j.advwatres.2009.05.006

Batjes, N. H. (2014). Total carbon and nitrogen in the soils of the world. *European Journal of Soil Science*, *65*(1), 4–21. https://doi.org/10.1111/ejss.12114_2

Battin, T. J., Luyssaert, S., Kaplan, L. A., Aufdenkampe, A. K., Richter, A., & Tranvik, L. J. (2009). The boundless carbon cycle. *Nature Geoscience*, *2*(9), 598–600. https://doi.org/10.1038/ngeo618

Bausenwein, U., Gattinger, A., Langer, U., Embacher, A., Hartmann, H.-P., Sommer, M., et al. (2008). Exploring soil microbial communities and soil organic matter: Variability and interactions in arable soils under minimum tillage practice. *Applied Soil Ecology*, *40*(1), 67–77. https://doi.org/10.1016/j.apsoil.2008.03.006

Benscoter, B. W., Greenacre, D., & Turetsky, M. R. (2015). Wildfire as a key determinant of peatland microtopography. *Canadian Journal of Forest Research*, *45*(8), 1132–1136. https://doi.org/10.1139/cjfr-2015-0028

Bernal, S., Lupon, A., Wollheim, W. M., Sabater, F., Poblador, S., & Martí, E. (2019). Supply, demand, and in-stream retention of dissolved organic carbon and nitrate during storms in mediterranean forested headwater streams. *Frontiers in Environmental Science*, *7*. https://doi.org/10.3389/fenvs.2019.00060

Beudert, B., Bässler, C., Thorn, S., Noss, R., Schröder, B., Dieffenbach-Fries, H., et al. (2015). Bark beetles increase biodiversity while maintaining drinking water quality. *Conservation Letters*, *8*(4), 272–281. https://doi.org/10.1111/conl.12153

Birkel, C., Broder, T., & Biester, H. (2017). Nonlinear and threshold-dominated runoff generation controls DOC export in a small peat catchment. *Journal of Geophysical Research: Biogeosciences*, *122*(3), 498–513. https://doi.org/10.1002/2016JG003621

Bishop, K. H., Seibert, J., Köhler, S. J., & Laudon, H. (2004). Resolving the Double Paradox of rapidly mobilized old water with highly variable responses in runoff chemistry. *Hydrological Processes*, *18*(1), 185–189. https://doi.org/10.1002/hyp.5209

Blaurock, K., Beudert, B., Gilfedder, B. S., Fleckenstein, J. H., Peiffer, S., & Hopp, L. (2021). Low hydrological connectivity after summer drought inhibits DOC export in a forested headwater catchment. *Hydrology and Earth System Sciences*, *25*(9), 5133–5151. https://doi.org/10.5194/hess-25-5133-2021

Blazejewski, G. A., Stolt, M. H., Gold, A. J., Gurwick, N., & Groffman, P. M. (2009). Spatial distribution of carbon in the subsurface of riparian zones. *Soil Science Society of America Journal*, *73*(5), 1733–1740. https://doi.org/10.2136/sssaj2007.0386

Bol, R., Lücke, A., Tappe, W., Kummer, S., Krause, M., Weigand, S., et al. (2015). Spatio-temporal variations of dissolved organic matter in a German forested mountainous headwater catchment. *Vadose Zone Journal*, *14*(4). https://doi.org/10.2136/vzj2015.01.0005

Borken, W., & Matzner, E. (2009). Reappraisal of drying and wetting effects on C and N mineralization and fluxes in soils. *Global Change Biology*, *15*(4), 808–824. https://doi.org/10.1111/j.1365-2486.2008.01681.x

Bormann, B. T., Spaltenstein, H., McClellan, M. H., Ugolini, F. C., Cromack, K., Jr., & Nay, S. M. (1995). Rapid soil development after windthrow disturbance in pristine forests. *Journal of Ecology*, *83*(5), 747–757. https://doi.org/10.2307/2261411

Broder, T., Knorr, K.-H., & Biester, H. (2017). Changes in dissolved organic matter quality in a peatland and forest headwater stream as a function of seasonality and hydrologic conditions. *Hydrology and Earth System Sciences*, *21*(4), 2035–2051. https://doi.org/10.5194/hess-21-2035-2017

Christophersen, N., Neal, C., Hooper, R. P., Vogt, R. D., & Andersen, S. (1990). Modeling stream water chemistry as a mixture of soil water end-members—A step towards second-generation acidification models. *Journal of Hydrology*, *116*(1–4), 307–320. https://doi.org/10.1016/0022-1694(90)90130-P

Clinton, B. D., & Baker, C. R. (2000). Catastrophic windthrow in the southern Appalachians: Characteristics of pits and mounds and initial vegetation responses. *Forest Ecology and Management*, *126*(1), 51–60. https://doi.org/10.1016/S0378-1127(99)00082-1

Cole, J. J., Prairie, Y. T., Caraco, N. F., McDowell, W. H., Tranvik, L. J., Striegl, R. G., et al. (2007). Plumbing the global carbon cycle: Integrating inland waters into the terrestrial carbon budget. *Ecosystems*, *10*(1), 172–185. https://doi.org/10.1007/s10021-006-9013-8

Corvasce, M., Zsolnay, A., D'Orazio, V., Lopez, R., & Miano, T. M. (2006). Characterization of water extractable organic matter in a deep soil profile. *Chemosphere*, *62*(10), 1583–1590. https://doi.org/10.1016/j.chemosphere.2005.07.065

Cory, N., Laudon, H., Köhler, S. J., Seibert, J., & Bishop, K. H. (2007). Evolution of soil solution aluminum during transport along a forested boreal hillslope. *Journal of Geophysical Research: Biogeosciences*, *112*(G3). https://doi.org/10.1029/2006JG000387

Cory, R. M., & McKnight, D. M. (2005). Fluorescence spectroscopy reveals ubiquitous presence of oxidized and reduced quinones in dissolved organic matter. *Environmental Science & Technology*, *39*(21), 8142–8149. https://doi.org/10.1021/es0506962

Courtwright, J., & Findlay, S. E. G. (2011). Effects of microtopography on hydrology, physicochemistry, and vegetation in a tidal swamp of the Hudson River. *Wetlands*, *31*(2), 239–249. https://doi.org/10.1007/s13157-011-0156-9

Creed, I. F., Sanford, S. E., Beall, F. D., Molot, L. A., & Dillon, P. J. (2003). Cryptic wetlands: Integrating hidden wetlands in regression models of the export of dissolved organic carbon from forested landscapes. *Hydrological Processes*, *17*(18), 3629–3648. https://doi.org/10.1002/hyp.1357

Cresto Aleina, F., Runkle, B. R. K., Kleinen, T., Kutzbach, L., Schneider, J., & Brovkin, V. (2015). Modeling micro-topographic controls on boreal peatland hydrology and methane fluxes. *Biogeosciences*, *12*(19), 5689–5704. https://doi.org/10.5194/bg-12-5689-2015

Curtinrich, H. J., Sebestyen, S. D., Griffiths, N. A., & Hall, S. J. (2021). Warming stimulates iron-mediated carbon and nutrient cycling in mineral-poor peatlands. *Ecosystems*, *25*, 44–60. https://doi.org/10.1007/s10021-021-00639-3

Dahlén, J., Bertilsson, S., & Pettersson, C. (1996). Effects of UV-A irradiation on dissolved organic matter in humic surface waters. *Environment International*, *22*(5), 501–506. https://doi.org/10.1016/0160-4120(96)00038-4

Da Silva, M. P., Blaurock, K., Beudert, B., Fleckenstein, J. H., Hopp, L., Peiffer, S., et al. (2021). Delineating source contributions to stream dissolved organic matter composition under baseflow conditions in forested headwater catchments. *Journal of Geophysical Research: Biogeosciences*, *126*(8). https://doi.org/10.1029/2021JG006425

Dawson, J. J. C., Soulsby, C., Tetzlaff, D., Hrachowitz, M., Dunn, S. M., & Malcolm, I. A. (2008). Influence of hydrology and seasonality on DOC exports from three contrasting upland catchments. *Biogeochemistry*, *90*(1), 93–113. https://doi.org/10.1007/s10533-008-9234-3

Detty, J. M., & McGuire, K. J. (2010). Threshold changes in storm runoff generation at a till-mantled headwater catchment. *Water Resources Research*, *46*(7), 1356. https://doi.org/10.1029/2009WR008102

Diamond, J. S., Epstein, J. M., Cohen, M. J., McLaughlin, D. L., Hsueh, Y.-H., Keim, R. F., & Duberstein, J. A. (2021). A little relief: Ecological functions and autogenesis of wetland microtopography. *WIREs Water*, *8*(1). https://doi.org/10.1002/wat2.1493

Dixon, R. K., Brown, S., Houghton, R. A., Solomon, A. M., Trexler, M. C., & Wisniewski, J. (1994). Carbon pools and flux of global forest ecosystems. *Science*, *263*(5144), 185–190. https://doi.org/10.1126/science.263.5144.185

Downing, J. A. (2012). Global abundance and size distribution of streams and rivers. *Inland Waters*, *2*(4), 229–236. https://doi.org/10.5268/IW-2.4.502

Drake, T. W., Raymond, P. A., & Spencer, R. G. M. (2018). Terrestrial carbon inputs to inland waters: A current synthesis of estimates and uncertainty. *Limnology and Oceanography Letters*, *3*(3), 132–142. https://doi.org/10.1002/lol2.10055

Evans, C. D., Chapman, P. J., Clark, J. M., Montheith, D., & Cresser, M. S. (2006). Alternative explanations for rising dissolved organic carbon export from organic soils. *Global Change Biology*, *12*(11), 2044–2053. https://doi.org/10.1111/j.1365-2486.2006.01241.x

Evans, C. D., Monteith, D. T., & Cooper, D. M. (2005). Long-term increases in surface water dissolved organic carbon: Observations, possible causes, and environmental impacts. *Environmental Pollution*, *137*(1), 55–71. https://doi.org/10.1016/j.envpol.2004.12.031

Fellman, J. B., Hood, E., Edwards, R. T., & D'Amore, D. V. (2009). Changes in the concentration, biodegradability, and fluorescent properties of dissolved organic matter during stormflows in coastal temperate watersheds. *Journal of Geophysical Research*, *114*(G1), G01021. https://doi.org/10.1029/2008JG000790

Findlay, S. E. G., Quinn, J. M., Hickey, C. W., Burrell, G., & Downes, M. (2001). Effects of land use and riparian flow path on delivery of dissolved organic carbon to streams. *Limnology & Oceanography*, *46*(2), 345–355. https://doi.org/10.4319/lo.2001.46.2.0345

Fitzgerald, D. F., Price, J. S., & Gibson, J. J. (2003). Hillslope-swamp interactions and flow pathways in a hypermaritime rainforest, British Columbia. *Hydrological Processes*, *17*(15), 3005–3022. https://doi.org/10.1002/hyp.1279

Fontaine, S., Barot, S., Barré, P., Bdioui, N., Mary, B., & Rumpel, C. (2007). Stability of organic carbon in deep soil layers controlled by fresh carbon supply. *Nature*, *450*(7167), 277–280. https://doi.org/10.1038/nature06275

Frei, S., Knorr, K.-H., Peiffer, S., & Fleckenstein, J. H. (2012). Surface micro-topography causes hot spots of biogeochemical activity in wetland systems: A virtual modeling experiment. *Journal of Geophysical Research: Biogeosciences*, *117*(G4). https://doi.org/10.1029/2012JG002012

Frei, S., Lischeid, G., & Fleckenstein, J. H. (2010). Effects of micro-topography on surface-subsurface exchange and runoff generation in a virtual riparian wetland —A modeling study. *Advances in Water Resources*, *33*(11), 1388–1401. https://doi.org/10.1016/j.advwatres.2010.07.006

Gilland, K. E., & McCarthy, B. C. (2014). Microtopography influences early successional plant communities on experimental coal surface mine land reclamation. *Restoration Ecology*, *22*(2), 232–239. https://doi.org/10.1111/rec.12066

Gomi, T., Sidle, R. C., Richardson, J. S., & John, S. (2002). Understanding processes and downstream linkages of headwater systems. *BioScience*, *52*(10), 905. https://doi.org/10.1641/0006-3568(2002)052[0905:UPADLO]2.0.CO;2

Grabs, T., Bishop, K. H., Laudon, H., Lyon, S. W., & Seibert, J. (2012). Riparian zone hydrology and soil water total organic carbon (TOC): Implications for spatial variability and upscaling of lateral riparian TOC exports. *Biogeosciences*, *9*(10), 3901–3916. https://doi.org/10.5194/bg-9-3901-2012

Grybos, M., Davranche, M., Gruau, G., Petitjean, P., & Pédrot, M. (2009). Increasing pH drives organic matter solubilization from wetland soils under reducing conditions. *Geoderma*, *154*(1–2), 13–19. https://doi.org/10.1016/j.geoderma.2009.09.001

Helms, J. R., Stubbin, A., Ritchie, J. D., Minor, E. C., Kieber, D. J., & Mopper, K. (2008). Absorption spectral slopes and slope ratios as indicators of molecular weight, source, and photobleaching of chromophoric dissolved organic matter. *Limnology & Oceanography*, *53*(3), 955–969. https://doi.org/10.4319/lo.2008.53.3.0955

Hongve, D., Riise, G., & Kristiansen, J. F. (2004). Increased color and organic acid concentrations in Norwegian forest lakes and drinking water? A result of increased precipitation? *Aquatic Sciences—Research Across Boundaries*, *66*(2), 231–238. https://doi.org/10.1007/s00027-004-0708-7

Hood, E., Gooseff, M. N., & Johnson, S. L. (2006). Changes in the character of stream water dissolved organic carbon during flushing in three small watersheds, Oregon. *Journal of Geophysical Research*, *111*(G1), 567. https://doi.org/10.1029/2005JG000082

Hruška, J., Krám, P., McDowell, W. H., & Oulehle, F. (2009). Increased dissolved organic carbon (DOC) in central European streams is driven by reductions in ionic strength rather than climate change or decreasing acidity. *Environmental Science & Technology*, *43*(12), 4320–4326. https://doi.org/10.1021/es803645w

Huguet, A., Vacher, L., Relexans, S., Saubusse, S., Froidefond, J. M., & Parlanti, E. (2009). Properties of fluorescent dissolved organic matter in the Gironde Estuary. *Organic Geochemistry*, *40*(6), 706–719. https://doi.org/10.1016/j.orggeochem.2009.03.002

Inamdar, S. P., & Mitchell, M. J. (2007). Contributions of riparian and hillslope waters to storm runoff across multiple catchments and storm events in a glaciated forested watershed. *Journal of Hydrology*, *341*(1–2), 116–130. https://doi.org/10.1016/j.jhydrol.2007.05.007

Jacks, G., & Norrström, A.-C. (2004). Hydrochemistry and hydrology of forest riparian wetlands. *Forest Ecology and Management*, *196*(2–3), 187–197. https://doi.org/10.1016/j.foreco.2004.01.055

Jaffé, R., McKnight, D. M., Maie, N., Cory, R. M., McDowell, W. H., & Campbell, J. L. (2008). Spatial and temporal variations in DOM composition in ecosystems: The importance of long-term monitoring of optical properties. *Journal of Geophysical Research: Biogeosciences*, *113*(G4). https://doi.org/10.1029/2008JG000683

Kalbitz, K., Solinger, S., Park, J.-H., Michalzik, B., & Matzner, E. (2000). Controls on the dynamics of dissolved organic matter in soils: A review. *Soil Science*, *165*(4), 277–304. https://doi.org/10.1097/00010694-200004000-00001

Karlsson, T., & Persson, P. (2012). Complexes with aquatic organic matter suppress hydrolysis and precipitation of Fe(III). *Chemical Geology*, *322–323*, 19–27. https://doi.org/10.1016/j.chemgeo.2012.06.003

Kawasaki, M., Ohte, N., & Katsuyama, M. (2005). Biogeochemical and hydrological controls on carbon export from a forested catchment in central Japan. *Ecological Research*, *20*(3), 347–358. https://doi.org/10.1007/s11284-005-0050-0

Kindler, R., Siemens, J., Kaiser, K., Walmsley David, C., Bernhofer, C., Buchmann, N., et al. (2011). Dissolved carbon leaching from soil is a crucial component of the net ecosystem carbon balance. *Global Change Biology*, *17*(2), 1167–1185. https://doi.org/10.1111/j.1365-2486.2010.02282.x

Knorr, K.-H. (2013). DOC-dynamics in a small headwater catchment as driven by redox fluctuations and hydrological flow paths—Are DOC exports mediated by iron reduction/oxidation cycles? *Biogeosciences*, *10*(2), 891–904. https://doi.org/10.5194/bg-10-891-2013

Koch, B. P., & Dittmar, T. (2006). From mass to structure: An aromaticity index for high-resolution mass data of natural organic matter. *Rapid Communications in Mass Spectrometry*, *20*(5), 926–932. https://doi.org/10.1002/rcm.2386

Koch, B. P., & Dittmar, T. (2016). From mass to structure: An aromaticity index for high-resolution mass data of natural organic matter. *Rapid Communications in Mass Spectrometry*, *30*(1), 250. https://doi.org/10.1002/rcm.7433

Kooch, Y., Hosseini, S. M., Samonil, P., & Hojjati, S. M. (2014). The effect of windthrow disturbances on biochemical and chemical soil properties in the northern mountainous forests of Iran. *Catena*, *116*, 142–148. https://doi.org/10.1016/j.catena.2014.01.002

Kothawala, D. N., Ji, X., Laudon, H., Ågren, A. M., Futter, M. N., Köhler, S. J., & Tranvik, L. J. (2015). The relative influence of land cover, hydrology, and in-stream processing on the composition of dissolved organic matter in boreal streams. *Journal of Geophysical Research: Biogeosciences*, *120*(8), 1491–1505. https://doi.org/10.1002/2015JG002946

Kuglerová, L., Jansson, R., Ågren, A. M., Laudon, H., & Malm-Renöfält, B. (2014). Groundwater discharge creates hotspots of riparian plant species richness in a boreal forest stream network. *Ecology*, *95*(3), 715–725. https://doi.org/10.1890/13-0363.1

Laudon, H., Berggren, M., Ågren, A. M., Buffam, I., Bishop, K. H., Grabs, T., et al. (2011). Patterns and dynamics of dissolved organic carbon (DOC) in boreal streams: The role of processes, connectivity, and scaling. *Ecosystems*, *14*(6), 880–893. https://doi.org/10.1007/s10021-011-9452-8

Laudon, H., Kuglerová, L., Sponseller, R. A., Futter, M., Nordin, A., Bishop, K., et al. (2016). The role of biogeochemical hotspots, landscape heterogeneity, and hydrological connectivity for minimizing forestry effects on water quality. *Ambio*, *45*(Suppl 2), 152–162. https://doi.org/10.1007/s13280-015-0751-8

Ledesma, J. L. J., Futter, M. N., Blackburn, M., Lidman, F., Grabs, T., Sponseller, R. A., et al. (2018). Towards an improved conceptualization of riparian zones in boreal forest headwaters. *Ecosystems*, *21*(2), 297–315. https://doi.org/10.1007/s10021-017-0149-5

Ledesma, J. L. J., Futter, M. N., Laudon, H., Evans, C. D., & Köhler, S. J. (2016). Boreal forest riparian zones regulate stream sulfate and dissolved organic carbon. *The Science of the Total Environment*, *560–561*, 110–122. https://doi.org/10.1016/j.scitotenv.2016.03.230

Ledesma, J. L. J., Grabs, T., Bishop, K. H., Schiff, S. L., & Köhler, S. J. (2015). Potential for long-term transfer of dissolved organic carbon from riparian zones to streams in boreal catchments. *Global Change Biology*, *21*(8), 2963–2979. https://doi.org/10.1111/gcb.12872

Ledesma, J. L. J., Köhler, S. J., & Futter, M. N. (2012). Long-term dynamics of dissolved organic carbon: Implications for drinking water supply. *The Science of the Total Environment*, *432*, 1–11. https://doi.org/10.1016/j.scitotenv.2012.05.071

Ledesma, J. L. J., Kothawala, D. N., Bastviken, P., Maehder, S., Grabs, T., & Futter, M. N. (2018). Stream dissolved organic matter composition reflects the riparian zone, not upslope soils in boreal forest headwaters. *Water Resources Research*, *54*(6), 3896–3912. https://doi.org/10.1029/2017WR021793

Leenheer, J. A., & Croué, J.-P. (2003). Characterizing aquatic dissolved organic matter. *Environmental Science & Technology*, *37*(1), 18A–26A. https://doi.org/10.1021/es032333c

Lessels, J. S., Tetzlaff, D., Birkel, C., Dick, J., & Soulsby, C. (2016). Water sources and mixing in riparian wetlands revealed by tracers and geospatial analysis. *Water Resources Research*, *52*(1), 456–470. https://doi.org/10.1002/2015WR017519

Lupon, A., Denfeld, B. A., Laudon, H., Leach, J., Karlsson, J., & Sponseller, R. A. (2019). Groundwater inflows control patterns and sources of greenhouse gas emissions from streams. *Limnology & Oceanography*, *64*(4), 1545–1557. https://doi.org/10.1002/lno.11134

Marschner, B., & Kalbitz, K. (2003). Controls of bioavailability and biodegradability of dissolved organic matter in soils. *Geoderma*, *113*(3–4), 211–235. https://doi.org/10.1016/S0016-7061(02)00362-2

Mastný, J., Kaštovská, E., Bárta, J., Chroňáková, A., Borovec, J., Šantrůčková, H., et al. (2018). Quality of DOC produced during litter decomposition of peatland plant dominants. *Soil Biology and Biochemistry*, *121*, 221–230. https://doi.org/10.1016/j.soilbio.2018.03.018

Mazzola, V., Perks, M. P., Smith, J., Yeluripati, J., & Xenakis, G. (2021). Seasonal patterns of greenhouse gas emissions from a forest-to-bog restored site in northern Scotland: Influence of microtopography and vegetation on carbon dioxide and methane dynamics. *European Journal of Soil Science*, *72*(3), 1332–1353. https://doi.org/10.1111/ejss.13050

McDowell, W. H., & Likens, G. E. (1988). Origin, composition, and flux of dissolved organic carbon in the Hubbard Brook valley. *Ecological Monographs*, *58*(3), 177–195. https://doi.org/10.2307/2937024

McGuire, K. J., & McDonnell, J. J. (2010). Hydrological connectivity of hillslopes and streams: Characteristic time scales and nonlinearities. *Water Resources Research*, *46*(10), 2010WR009341. https://doi.org/10.1029/2010WR009341

McKnight, D. M., Boyer, E. W., Westerhoff, P., Doran, P. T., Kulbe, T., & Dale, T. A. (2001). Spectrofluorometric characterization of dissolved organic matter for indication of precursor organic material and aromaticity. *Limnology & Oceanography*, *46*(1), 38–48. https://doi.org/10.4319/lo.2001.46.1.0038

Mehra, O. P., & Jackson, M. L. (1958). Iron oxide removal from soils and clays by a dithionite-citrate system buffered with sodium bicarbonate. *Clays and Clay Minerals*, *7*, 317–327. https://doi.org/10.1016/B978-0-08-009235-5.50026-7

Mei, Y., Hornberger, G. M., Kaplan, L. A., Newbold, J. D., & Aufdenkampe, A. K. (2014). The delivery of dissolved organic carbon from a forested hillslope to a headwater stream in southeastern Pennsylvania, USA. *Water Resources Research*, *50*(7), 5774–5796. https://doi.org/10.1002/2014WR015635

Minick, K. J., Kelley, A. M., Miao, G., Li, X., Noormets, A., Mitra, B., & King, J. S. (2019). Microtopography alters hydrology, phenol oxidase activity and nutrient availability in organic soils of a coastal freshwater forested wetland. *Wetlands*, *39*(2), 263–273. https://doi.org/10.1007/s13157-018-1107-5

Monteith, D. T., Stoddard, J. L., Evans, C. D., de Wit, H. A., Forsius, M., Høgåsen, T., et al. (2007). Dissolved organic carbon trends resulting from changes in atmospheric deposition chemistry. *Nature*, *450*(7169), 537–540. https://doi.org/10.1038/nature06316

Moser, K. F., Ahn, C., & Noe, G. B. (2009). The influence of microtopography on soil nutrients in created mitigation wetlands. *Restoration Ecology*, *17*(5), 641–651. https://doi.org/10.1111/j.1526-100X.2008.00393.x

Musolff, A., Fleckenstein, J. H., Opitz, M., Büttner, O., Kumar, R., & Tittel, J. (2018). Spatio-temporal controls of dissolved organic carbon stream water concentrations. *Journal of Hydrology*, *566*, 205–215. https://doi.org/10.1016/j.jhydrol.2018.09.011

Musolff, A., Selle, B., Büttner, O., Opitz, M., & Tittel, J. (2016). Unexpected release of phosphate and organic carbon to streams linked to declining nitrogen depositions. *Global Change Biology*, *23*(5), 1891–1901. https://doi.org/10.1111/gcb.13498

Nguyen, H. V.-M., Hur, J., & Shin, H.-S. (2010). Changes in spectroscopic and molecular weight characteristics of dissolved organic matter in a river during a storm event. *Water, Air, & Soil Pollution*, *212*(1–4), 395–406. https://doi.org/10.1007/s11270-010-0353-9

Nguyen, H. V.-M., Lee, M.-H., Hur, J., & Schlautman, M. A. (2013). Variations in spectroscopic characteristics and disinfection byproduct formation potentials of dissolved organic matter for two contrasting storm events. *Journal of Hydrology*, *481*, 132–142. https://doi.org/10.1016/j.jhydrol.2012.12.044

Nieminen, M., Koskinen, M., Sarkkola, S., Laurén, A., Kaila, A., Kiikkilä, O., et al. (2015). Dissolved organic carbon export from harvested peatland forests with differing site characteristics. *Water, Air, & Soil Pollution*, *226*(6), 101. https://doi.org/10.1007/s11270-015-2444-0

Nungesser, M. K. (2003). Modeling microtopography in boreal peatlands: Hummocks and hollows. *Ecological Modeling*, *165*(2), 175–207. https://doi.org/10.1016/S0304-3800(03)00067-X

Ohno, T. (2002). Fluorescence inner-filtering correction for determining the humification index of dissolved organic matter. *Environmental Science & Technology*, *36*(4), 742–746. https://doi.org/10.1021/es0155276

Palmer, S. M., Wellington, B. I., Johnson, C. E., & Driscoll, C. T. (2005). Landscape influences on aluminum and dissolved organic carbon in streams draining the Hubbard Brook valley, New Hampshire, USA. *Hydrological Processes*, *19*(9), 1751–1769. https://doi.org/10.1002/hyp.5660

Pan, W., Kan, J., Inamdar, S. P., Chen, C., & Sparks, D. (2016). Dissimilatory microbial iron reduction release DOC (dissolved organic carbon) from carbon-ferrihydrite association. *Soil Biology and Biochemistry*, *103*, 232–240. https://doi.org/10.1016/j.soilbio.2016.08.026

Park, H., & Kim, J. G. (2020). Temporal and spatial variations of vegetation in a riparian zone of South Korea. *Journal of Ecology and Environment*, *44*(1), 9. https://doi.org/10.1186/s41610-020-00152-z

Parlanti, E., Wörz, K., Geoffroy, L., & Lamotte, M. (2000). Dissolved organic matter fluorescence spectroscopy as a tool to estimate biological activity in a coastal zone submitted to anthropogenic inputs. *Permafrost and Periglacial Processes*, *31*(12), 1765–1781. https://doi.org/10.1016/S0146-6380(00)00124-8

Peiffer, S., Walton-Day, K., & Macalady, D. L. (1999). The interaction of natural organic matter with iron in a wetland (Tennessee Park, Colorado) receiving acid mine drainage. *Aquatic Geochemistry*, *5*(2), 207–223. https://doi.org/10.1023/a:1009617925959

Pellerin, B. A., Fernandez, I. J., Norton, S. A., & Kahl, J. S. (2002). Soil aluminum distribution in the near-stream zone at the bear Brook watershed in Maine. *Water, Air, and Soil Pollution*, *134*(1/4), 189–204. https://doi.org/10.1023/a:1014115717784

Penna, D., van Meerveld, H. J., Oliviero, O., Zuecco, G., Assendelft, R. S., Dalla Fontana, G., & Borga, M. (2015). Seasonal changes in runoff generation in a small forested mountain catchment. *Hydrological Processes*, *29*(8), 2027–2042. https://doi.org/10.1002/hyp.10347

Pisani, O., Bosch, D. D., Coffin, A. W., Endale, D. M., Liebert, D., & Strickland, T. C. (2020). Riparian land cover and hydrology influence stream dissolved organic matter composition in an agricultural watershed. *The Science of the Total Environment*, *717*, 137165. https://doi.org/10.1016/j.scitotenv.2020.137165

Ploum, S. W., Laudon, H., Peralta-Tapia, A., & Kuglerová, L. (2020). Are dissolved organic carbon concentrations in riparian groundwater linked to hydrological pathways in the boreal forest? *Hydrology and Earth System Sciences*, *24*(4), 1709–1720. https://doi.org/10.5194/hess-24-1709-2020

Ploum, S. W., Leach, J. A., Laudon, H., & Kuglerová, L. (2021). Groundwater, soil, and vegetation interactions at discrete riparian inflow points (DRIPs) and implications for boreal streams. *Frontiers in Water*, *3*. https://doi.org/10.3389/frwa.2021.669007

Poulin, B. A., Ryan, J. N., & Aiken, G. R. (2014). Effects of iron on optical properties of dissolved organic matter. *Environmental Science & Technology*, *48*(17), 10098–10106. https://doi.org/10.1021/es502670r

Raymond, P. A., Hartmann, J., Lauerwald, R., Sobek, S., McDonald, C., Hoover, M., et al. (2013). Global carbon dioxide emissions from inland waters. *Nature*, *503*(7476), 355–359. https://doi.org/10.1038/nature12760

Raymond, P. A., & Saiers, J. E. (2010). Event controlled DOC export from forested watersheds. *Biogeochemistry*, *100*(1–3), 197–209. https://doi.org/10.1007/s10533-010-9416-7

Raymond, P. A., Saiers, J. E., & Sobczak, W. V. (2016). Hydrological and biogeochemical controls on watershed dissolved organic matter transport: Pulse-shunt concept. *Ecology*, *97*(1), 5–16. https://doi.org/10.1890/14-1684.1

Riedel, T., Biester, H., & Dittmar, T. (2012). Molecular fractionation of dissolved organic matter with metal salts. *Environmental Science & Technology*, *46*(8), 4419–4426. https://doi.org/10.1021/es203901u

Rogers, D. B., Newcomer, M. E., Raberg, J. H., Dwivedi, D., Steefel, C., Bouskill, N., et al. (2021). Modeling the impact of riparian hollows on river corridor nitrogen exports. *Frontiers in Water*, *3*. https://doi.org/10.3389/frwa.2021.590314

Roulet, N., & Moore, T. R. (2006). Browning the waters. *Nature*, *444*(7117), 283–284. https://doi.org/10.1038/444283a

Sadiq, R., & Rodriguez, M. J. (2004). Disinfection by-products (DBPs) in drinking water and predictive models for their occurrence: A review. *The Science of the Total Environment*, *321*(1–3), 21–46. https://doi.org/10.1016/j.scitotenv.2003.05.001

Scheliga, B., Tetzlaff, D., Nuetzmann, G., & Soulsby, C. (2019). Assessing runoff generation in riparian wetlands: Monitoring groundwater-surface water dynamics at the micro-catchment scale. *Environmental Monitoring and Assessment*, *191*(2), 116. https://doi.org/10.1007/s10661-019-7237-2

Schwarze, R., & Beudert, B. (2009). Analyse der Hochwassergenese und des Wasserhaushalts eines bewaldeten Einzugsgebietes unter dem Einfluss eines massiven Borkenkäferbefalls. *Hydrologie und Wasserbewirtschaftung*, *53*(4), 236–249.

Seibert, J., Grabs, T., Köhler, S. J., Laudon, H., Winterdahl, M., & Bishop, K. H. (2009). Linking soil- and stream-water chemistry based on a riparian flow-concentration integration model. *Hydrology and Earth System Sciences*, *13*(12), 2287–2297. https://doi.org/10.5194/hess-13-2287-2009

Selle, B., Knorr, K.-H., & Lischeid, G. (2019). Mobilization and transport of dissolved organic carbon and iron in peat catchments—Insights from the Lehstenbach stream in Germany using generalized additive models. *Hydrological Processes*, *33*(25), 3213–3225. https://doi.org/10.1002/hyp.13552

Spencer, R. G. M., Aiken, G. R., Wickland, K. P., Striegl, R. G., & Hernes, P. J. (2008). Seasonal and spatial variability in dissolved organic matter quantity and composition from the Yukon River basin, Alaska. *Global Biogeochemical Cycles*, *22*(4). https://doi.org/10.1029/2008GB003231

Stevenson, C., Filicetti, A., & Nielsen, S. (2019). High precision altimeter demonstrates simplification and depression of microtopography on seismic lines in treed peatlands. *Forests*, *10*(4), 295. https://doi.org/10.3390/f10040295

Stoeckel, D. M., & Miller-Goodman, M. S. (2001). Seasonal nutrient dynamics of forested floodplain soil influenced by microtopography and depth. *Soil Science Society of America Journal*, *65*(3), 922–931. https://doi.org/10.2136/sssaj2001.653922x

Strohmeier, S., Knorr, K.-H., Reichert, M., Frei, S., Fleckenstein, J. H., Peiffer, S., & Matzner, E. (2013). Concentrations and fluxes of dissolved organic carbon in runoff from a forested catchment: Insights from high-frequency measurements. *Biogeosciences*, *10*(2), 905–916. https://doi.org/10.5194/bg-10-905-2013

Tamura, H., Goto, K., Yotsuyanagi, T., & Nagayama, M. (1974). Spectrophotometric determination of iron(II) with 1, 10-phenanthroline in the presence of large amounts of iron(III). *Talanta*, *21*(4), 314–318. https://doi.org/10.1016/0039-9140(74)80012-3

Ulanova, N. G. (2000). The effects of windthrow on forests at different spatial scales: A review. *Forest Ecology and Management*, *135*(1–3), 155–167. https://doi.org/10.1016/S0378-1127(00)00307-8

Vidon, P. G. (2017). Not all riparian zones are wetlands: Understanding the limitation of the "wetland bias" problem. *Hydrological Processes*, *31*(11), 2125–2127. https://doi.org/10.1002/hyp.11153

Vidon, P. G., & Hill, A. R. (2004). Landscape controls on the hydrology of stream riparian zones. *Journal of Hydrology*, *292*(1–4), 210–228. https://doi.org/10.1016/j.jhydrol.2004.01.005

Vidon, P. G., Wagner, L. E., & Soyeux, E. (2008). Changes in the character of DOC in streams during storms in two Midwestern watersheds with contrasting land uses. *Biogeochemistry*, *88*(3), 257–270. https://doi.org/10.1007/s10533-008-9207-6

Vogt, R. D., & Muniz, I. P. (1997). Soil and stream water chemistry in a pristine and boggy site in mid-Norway. *Hydrobiologia*, *348*(1/2/3), 19–38. https://doi.org/10.1023/a:1003029031653

Wagner, S., Fair, J. H., Matt, S., Hosen, J. D., Raymond, P. A., Saiers, J., et al. (2019). Molecular hysteresis: Hydrologically driven changes in riverine dissolved organic matter chemistry during a storm event. *Journal of Geophysical Research: Biogeosciences*, *124*(4), 759–774. https://doi.org/10.1029/2018JG004817

Weishaar, J. L., Aiken, G. R., Bergamaschi, B. A., Fram, M. S., Fujii, R., & Mopper, K. (2003). Evaluation of specific ultraviolet absorbance as an indicator of the chemical composition and reactivity of dissolved organic carbon. *Environmental Science & Technology*, *37*(20), 4702–4708. https://doi.org/10.1021/es030360x

Werner, B. J., Lechtenfeld, O. J., Musolff, A., de Rooij, G. H., Yang, J., Gründling, R., et al. (2021). Small-scale topography explains patterns and dynamics of dissolved organic carbon exports from the riparian zone of a temperate, forested catchment. *Hydrology and Earth System Sciences*, *25*(12), 6067–6086. https://doi.org/10.5194/hess-25-6067-2021

Weyhenmeyer, G. A., & Karlsson, J. (2009). Nonlinear response of dissolved organic carbon concentrations in boreal lakes to increasing temperatures. *Limnology & Oceanography*, *54*(6part2), 2513–2519. https://doi.org/10.4319/lo.2009.54.6_part_2.2513

Wohl, E. (2017). The significance of small streams. *Frontiers of Earth Science*, *11*(3), 447–456. https://doi.org/10.1007/s11707-017-0647-y

Xu, B., Li, J., Huang, Q., Gong, Q., & Li, L. (2016). Impacts of land use patterns and typhoon-induced heavy rainfall event on dissolved organic matter properties in the South Tiaoxi River, China. *Environmental Earth Sciences*, *75*(8), 632. https://doi.org/10.1007/s12665-016-5413-z

Zajac, E., Zarzycki, J., & Ryczek, M. (2018). Degradation of peat surface on an abandoned post-extracted bog and implications for re-vegetation. *Applied Ecology and Environmental Research*, *16*(3), 3363–3380. https://doi.org/10.15666/aeer/1603_33633380

References From the Supporting Information

Da Silva, M. P., Kaesler, J. M., Reemtsma, T., & Lechtenfeld, O. J. (2020). Absorption mode spectral processing improves data quality of natural organic matter analysis by Fourier-transform ion cyclotron resonance mass spectrometry. *Journal of the American Society for Mass Spectrometry*, *31*(7), 1615–1618. https://doi.org/10.1021/jasms.0c00138

Dittmar, T., Koch, B. P., Hertkorn, N., & Kattner, G. (2008). A simple and efficient method for the solid-phase extraction of dissolved organic matter (SPE-DOM) from seawater. *Limnology & Oceanography*, *6*(6), 230–235. https://doi.org/10.4319/lom.2008.6.230

Herzsprung, P., Hertkorn, N., Tümpling, W., von Harir, M., Friese, K., & Schmitt-Kopplin, P. (2014). Understanding molecular formula assignment of Fourier transform ion cyclotron resonance mass spectrometry data of natural organic matter from a chemical point of view. *Analytical and Bioanalytical Chemistry*, *406*(30), 7977–7987. https://doi.org/10.1007/s00216-014-8249-y

Kind, T., & Fiehn, O. (2007). Seven Golden Rules for heuristic filtering of molecular formulas obtained by accurate mass spectrometry. *BMC Bioinformatics*, *8*(1), 105. https://doi.org/10.1186/1471-2105-8-105

Koch, B. P., Kattner, G., Witt, M., & Passow, U. (2014). Molecular insights into the microbial formation of marine dissolved organic matter: Recalcitrant or labile? *Biogeosciences*, *11*(15), 4173–4190. https://doi.org/10.5194/bg-11-4173-2014

Raeke, J., Lechtenfeld, O. J., Wagner, M., Herzsprung, P., & Reemtsma, T. (2016). Selectivity of solid phase extraction of freshwater dissolved organic matter and its effect on ultrahigh resolution mass spectra. *Environmental Sciences: Processes & Impacts*, *18*(7), 918–927. https://doi.org/10.1039/C6EM00200E